LUND UNIVERSITY
Faculty of Science

Ensemble Green's function theory for interacting electrons with degenerate ground states

Erik Linnér

Thesis submitted for the degree of Master of Science
Project duration: 8 months

Supervised by Prof. Ferdi Aryasetiawan and Tor Sjöstrand

Department of Physics
Division of Mathematical Physics
May 2019

Abstract

An *ensemble Green's function theory* for many-electron systems with degenerate ground states, based on the von Neumann density matrix formalism, is proposed. The formalism is constructed without an assumption of an adiabatic connection. An ensemble analogue of Hedin's equations and the *GW Approximation* (GWA) is constructed. The formalism is applied to four model systems within GWA: a three-orbital Hubbard model, a two-dimensional harmonic oscillator, an Ising model with a triangular lattice and a hydrogen-like system, with comparison to the exact solutions. The response function and the Green's function are found to be in reasonable agreement with the exact result for the majority of the models. However, peaks originating from the non-interacting degenerate subspace are found to be routinely neglected in the response function by our employed one-shot computational approach. Furthermore, the relation between the finite-temperature Green's function theory and the proposed theory is studied, and an extension of the finite-temperature formalism to include electronic systems with degenerate states is proposed.

Acknowledgements

I want to express my deepest gratitude to my supervisor Prof. Ferdi Aryasetiawan; it was through his guidance, support and fruitful discussions this Master's thesis was completed. Furthermore, I would like to express my gratitude to my co-supervisor Tor Sjöstrand for his useful comments and discussions over the course of the project. For friendly and helpful discussions regarding electronic structure, I would like to thank the remaining members of the electronic structure group. Special thanks to Dr. Fredrik Nilsson and Viktor Christiansson, with the latter contributing with useful comments and proofreading on earlier drafts of this thesis. Outside the electronic structure group, I would like express my gratitude to Prof. Silke Biermann for helpful remarks on a late draft of this thesis. As a final expression of gratitude, I would like to thank my office mate Maitane Muñoz Basagoiti for detailed proofreading of early drafts of this thesis.

List of Abbreviations

CI	Configuration Interaction
CC	Coupled Cluster
DFT	Density Functional Theory
MBPT	Many-Body Perturbation Theory
LDA	Local Density Approximation
SIC	Self Interaction Correction
DMFT	Dynamical Mean-Field Theory
QSGW	Quasiparticle Self-consistent GW
GWA	GW-Approximation
PES	PhotoEmission Spectroscopy
IPES	Inverse PhotoEmission Spectroscopy
ARPES	Angle-Resolved PhotoEmission Spectroscopy
RPA	Random-Phase Approximation
MFT	Mean-Field Theory

Contents

Chapter 1

Introduction

The interaction between electrons is described by a pairwise interaction governed by one of the fundamental forces of nature: *electromagnetism*. A system composed of many such electrons, all interacting via the pairwise electron-electron interaction, is called a *many-electron system* or *electronic system*. An electronic system can contain a *degenerate* ground state, i.e. several states of the system having an identical energy equal to the lowest energy of the system. In nature, many electronic systems containing degenerate ground states exist, with examples ranging from open-shell atoms and molecules to vacancies in solids and two-dimensional electronic systems. Degenerate ground states may appear in *frustrated systems*, such as *frustrated magnets*. These systems are defined by that each pairwise interaction cannot, from the symmetry of the system, be satisfied at the same time. An example of a model of a frustrated magnet is the Ising model with a triangular lattice. Various fascinating and intriguing phenomena can originate from the ground state degeneracy. Prominent examples are the Landau degeneracy in two-dimensional electronic systems causing the fractional and integer quantum Hall effect [1] and the macroscopic degeneracy of the ground state in *spin ice*, a frustrated ferromagnet, leading to the appearance of magnetic monopoles [2]. Spin ice is a material composed of corner-sharing tetrahedra of magnetic ions, exhibiting a disorder of the magnetic moments analogous to the disorder of protons in water ice at low temperatures [3]. To describe such phenomena of electronic systems with degenerate ground states, one is required to employ a theory which incorporates the aspect of degeneracy.

The simple pairwise electron-electron interaction between all electrons lead to the emergance of complex and collective phenomena in electronic systems. A goal in the fields of Condensed Matter Physics and Quantum Chemistry is to simulate such electronic systems capturing the most important electronic properties. One approach is based on models with input parameters chosen to reproduce experimental data. This approach can be used to decipher the underlying physical mechanisms of phenomena in materials. However, the predictive power of these models is limited. The other approach is the *ab initio*, or *first principle*, approach, based on computing the electronic structure from only the structure of a material or molecule, i.e. only with the knowledge of charge and position of nuclei as well as the number of electrons, without adjustable parameters. While this approach has greater predictive power, it is more computationally demanding. Our considerations are of the first principle approach for electronic structure computations.

The non-relativistic quantum mechanics of interacting electrons in a many-electron system are exactly described by the Schrödinger equation and the given many-electron Hamiltonian. Thus, solving the Schrödinger equation in the case of many-electron systems

would in theory give the exact wavefunctions and eigenenergies, containing all information describing the system. However, it proves difficult to solve the Schrödinger equation exactly. In general, the properties of an electronic system cannot be solved for analytically, and in realistic systems the larger numbers of electrons makes solving it exactly unfeasible. The difficulty arises from the electron-electron interaction leading to every electron being correlated to all other electrons. Appropriate approximations and algorithms which capture the most important features of the electron correlation are thus required in the ab initio approach.

Several ab initio electronic structure computational approaches have been developed over the last half of the previous century until today. In small finite systems, such as atoms and small molecules, rigorous wave-function based computational methods such as *Configurational Interaction* (CI) and *Coupled Cluster* (CC) techniques are used for benchmark results. For large systems, wave-function based methods become increasingly computationally demanding and different approaches are required. In these systems, with examples such as solids and large molecules, there are two main categories of approaches: *Density Functional Theory* (DFT) and *Many-Body Perturbation Theory* (MBPT) based approaches. In DFT one maps the many-electron problem to a simple one-electron problem with an effective potential, the *Kohn-Sham potential*, giving the ground state properties of the system. In the DFT approach, a common starting point is the *Local Density Approximation* (LDA) [4, 5] which is based on the electron gas and expected to be suitable for delocalized electrons. For systems with electrons of a localized nature, i.e. a short-range correlation, LDA does not always work well. Examples of materials with short-range correlation are those containing atoms with valence electrons in 3d and 4f orbitals. Methods such as the LDA+U method [6, 7, 8] and the *Self Interaction Correction* (SIC) method [9] modify the LDA method to include a treatment of the localized nature of electrons. A current standard approach for treating systems with short-range correlation is LDA+DMFT [10, 11] which combines LDA with *Dynamical Mean-Field Theory* (DMFT), which is based on mapping a lattice model onto a quantum impurity model coupled to a reservoir [12, 13]. The exact Kohn-Sham eigenvalues obtained in DFT have no relation to the one-electron excitation energies of an electronic system, the *quasiparticle* energies, as these are related to excited state properties of the system. However, even without theoretical justification, the Kohn-Sham eigenvalues are usually taken as corresponding to the quasiparticle energies, since the agreement is good for a wide range of systems. A proper way to compute the one-electron excitation spectra and quasiparticle energies is through approaches based on *Green's function theory*, used in MBPT. In the Green's function approach, a common starting point is the one-shot G^0W^0 approach, corresponding to the first iteration of the self-consistent GW approach [14, 15]. The G^0W^0 scheme describes long-range correlation, and while quasiparticle energies are well-defined, the approach is more computationally demanding than the simpler LDA-approach. Furthermore, another example of a self-consistent approach is the *Quasiparticle Self-consistent GW* (QSGW) [16]. For systems with short-range correlation, one possible approach is the *GW+DMFT* approach, combining GW and DMFT [17]. Our work is focused on the Green's function theory and the G^0W^0 and GW approaches.

The Green's function theory approach is a well-established ab-initio approach for the compution of electronic properties of electronic systems with non-degenerate ground states. The approach is used for accurate calculations for systems of non-degenerate ground states as well as for systems of degenerate ground states. For the degenerate case at zero temperature, however, the standard approach is to either ignore the degeneracy

[18, 19] or to consider the degeneracy in a non-generalizable approach [20, 21]. This is required because, while DFT has been extended to degenerate ground states, a general zero-temperature Green's function formalism for degenerate ground states is not currently available. The difficulty of constructing a Green's function theory incorporating degenerate ground states originates from the common assumption of an *adiabatic connection* between an interacting ground state and a non-interacting ground state. In the case of degenerate non-interacting ground states, this connection is no longer obvious.

The history of attemps to extend the Green's function theory to the degenerate case begins at least as early as the 1960's. An early attempt of constructing a Green's function theory incorporating degenerate ground states is by Layzer in 1962, with the introduction of a *statistical* Green's function [22]. Another early attempt at extending the Green's function theory to electronic systems of degenerate ground states is by Cederbaum *et al* in the 1970's, with considerations of open-shell atoms and molecules [23]. Recently, C. Brouder *et al* have developed an alternative Green's function approach for degenerate ground states built upon nonperturbative adiabatic-approximation [24].

The main purpose of this thesis is to construct a general zero-temperature Green's function formalism incorporating the aspect of ground state degeneracy. We propose an *ensemble Green's function* theory based on the von Neumann density matrix formalism. The formalism is developed without an assumption of an adiabatic connection between interacting ground states and non-interacting ground states. Ensemble analogues of the *Hedin's equations* and the *GW-Approximation* (GWA) are developed. Based on the ensemble Hedin's equations, a one-shot and a self-consistent computational scheme for computation of the ensemble Green's function within ensemble GWA are constructed. To illustrate the scheme, four simple models with degenerate ground states are studied using the proposed formalism: a three-orbital Hubbard model, a two-dimensional harmonic oscillator model, an Ising model with a triangular lattice and a hydrogen-like system. The results of the ensemble approach are compared to the exact solutions. The relationship between the finite-temperature Green's function theory and the proposed ensemble formalism is studied. An extension of the temperature formalism to include electronic system with degenerate ground and/or excited states is further proposed.

This thesis is organized as follows. Chapter 2 is a theoretical background for the concepts treated in the thesis. The zero-temperature Green's function formalism for a non-degenerate ground state and the density matrix formalism are reviewed and a brief description of the finite-temperature Green's function formalism is given. Chapter 3 gives a definition of the proposed ensemble Green's function and a corresponding formalism is derived. Thereafter, an ensemble analogue of the Hedin's equations and GWA is developed. A one-shot and a self-consistent computational scheme within GWA is constructed. A study of the relationship between the temperature formalism and ensemble formalism, and a proposed extension of the temperature formalism for systems of degenerate states ends the chapter. Chapter 4 compiles the application of the constructed one-shot computational scheme to four simple model systems, with a comparison to the exact case and the case of neglecting the ground states degeneracy. In Chapter 5 the main conclusions of the thesis are summarized. In Chapter 6 an outlook for future developments and applications is given.

Chapter 2

Theoretical background

The main purpose of the current chapter is to establish the standard Green's function theory for the zero-temperature electron Green's function and the density matrix formalism, which our proposed ensemble Green's function formalism is built upon. An introduction to many-electron systems and the density matrix formalism begins the chapter. The equivalent *Schrödinger*, *Heisenberg* and *interaction pictures*, and the related adiabatic connection are then reviewed. Thereafter, a description of the linear response theory and the Kubo formula is given. The zero-temperature Green's function formalism is then reviewed by defining it and then developing it in detail by the use of the *Schwinger functional derivative technique*. The chapter ends with a short review of the finite-temperature Green's function theory.

2.1 Many-electron systems

In the field of electronic structure computation, the system under consideration is the many-electron system. The behavior of a many-electron system in the non-relativistic case is described by the well-known time-independent Schrödinger equation, using atomic units ($\hbar = m_e = 1$),

$$\hat{H}|\Psi_n\rangle = E_n|\Psi_n\rangle, \tag{2.1}$$

with the many-electron Hamiltonian:

$$\begin{aligned}\hat{H} = &\int dr\hat{\psi}^\dagger(r)h_0(r)\hat{\psi}(r) + \frac{1}{2}\int drdr'\hat{\psi}^\dagger(r)\hat{\psi}^\dagger(r')v(r-r')\hat{\psi}(r')\hat{\psi}(r) \\ &+ \int dr\hat{\psi}^\dagger(r)\varphi(r)\hat{\psi}(r),\end{aligned} \tag{2.2}$$

written in the field operator form and using the combined space and spin coordinate $r = (\vec{r}, \sigma)$. In the Hamiltonian, the first term, $h_0(r)$, is composed of contributions from the kinetics and the local potential experienced by the electrons, e.g. from a surrounding crystal lattice of nuclei; the second term, $v(r - r')$, is the electron-electron interaction; the third term, $\varphi(r)$, is the external potential. Relativistic effects are neglected and the local potential is assumed to be time-independent, e.g. the nuclei are considered fixed, thus neglecting electron-phonon interactions. The field operators are of the form:

$$\hat{\psi}(r) \equiv \sum_n \phi_n(r)\hat{c}_n, \quad \hat{\psi}^\dagger(r) \equiv \sum_n \phi_n^*(r)\hat{c}_n^\dagger, \tag{2.3}$$

with the orbital ϕ_n, and electron creation and annihilation operator $\hat{c}_n^\dagger$ and $\hat{c}_n$, respectively, for a one-electron state specified by n. Electrons obey Fermi-Dirac statistics and thus the creation and annihilation operators satisfy the anti-commutation relations:

$$\{\hat{c}_n, \hat{c}_m^\dagger\} = \delta_{nm}, \quad \{\hat{c}_n, \hat{c}_m\} = \{\hat{c}_n^\dagger, \hat{c}_m^\dagger\} = 0, \tag{2.4}$$

with Kronecker delta δ_{nm} defined as 1 for $n = m$ and 0 for $n \neq m$.

In general, Eq. (2.1) is not analytically solvable for an electronic system, and numerical methods are thus required. Appropriate approximations and computational schemes have therefore been developed. In the current thesis we specifically consider the Green's function theory within MBPT, with computational approaches within the GWA, an approximation first proposed by L. Hedin [14].

2.2 Density matrix

A physical system can be described as a statistical ensemble of a collection of systems occupying different states. A collection of systems all characterized by the same state $|\alpha\rangle$ defines a *pure ensemble*. In a *mixed ensemble* a fraction w_i of the systems are characterized by the state $|\alpha_i\rangle$, with i specifying different states. To describe such physical systems with pure or mixed ensembles one can use the density matrix formalism, originally introduced by von Neumann. For an in-depth review of the concept see for example [25].

All physically significant information related to the ensemble is stored in the density matrix $\hat{D}$, defined as

$$\hat{D} \equiv \sum_{i=1}^{M} w_i |\Phi_i\rangle\langle\Phi_i|, \quad \sum_{i=1}^{M} w_i = 1, \quad 0 \leq w_i \leq 1, \tag{2.5}$$

where $\{|\Phi_i\rangle, i = 1, ..., M\}$ is the set of M states spanning the Hilbert space of the system and with the corresponding fraction w_i specifying the ensemble uniquely. The states $\{|\Phi_i\rangle, i = 1, ..., M\}$ are not necessarily orthogonal. The ensemble average of any operator can within the density matrix formalism be written as

$$O \equiv \sum_{i=1}^{M} w_i \langle\Phi_i|\hat{O}|\Phi_i\rangle = Tr(\hat{D}\hat{O}). \tag{2.6}$$

For repeated measurements of a quantity, the average of the quantity corresponds to the ensemble average, i.e. the density matrix stores all information of physical significance in an ensemble. As an illustration, consider the ensemble average density given by:

$$\rho(r) = \sum_{i=1}^{M} w_i \langle\Phi_i|\hat{\rho}(r)|\Phi_i\rangle = \sum_{i=1}^{M} w_i \rho_i(r). \tag{2.7}$$

The structure of the proposed ensemble Green's function theory in section 3.1 will be based on the structure of the ensemble density.

2.3 Pictures

The Schrödinger, Heisenberg and interaction (Dirac) pictures, are three equivalent formulations of Quantum Mechanics. The pictures specify the time-dependence of the operators

and states, with the requirement that the expectation value of any operator is independent of the choice of picture. As observables are expectation values of operators, the three pictures describe identical observations. In our development of the Green's function theory based on MBPT, a time-dependent perturbation theory, both the Heisenberg and interaction pictures will be employed. For an in-depth review of the concepts see for example [26].

In the Schrödinger picture, operators are by definition time-independent and the states are time-dependent. In the Heisenberg picture, operators are instead time-dependent and the states are time-independent. The two pictures are related by the time-evolution operator

$$\hat{U}(t,t') = e^{-i\hat{H}(t-t')} \ , \tag{2.8}$$

where the function of an operator is defined as the Taylor expansion of the function. The two pictures coincide at $t = 0$, i.e.

$$\hat{O}_H(t) \equiv \hat{U}(t,0)\hat{O}_S\hat{U}(0,t) \ , \ \ |\Psi(t)\rangle_S \equiv \hat{U}(t,0)|\Psi\rangle_H \ , \tag{2.9}$$

where H and S labels the states and operators in the Heisenberg and Schrödinger picture, respectively. Notice that the expectation value of any operator is independent of the two pictures as required.

In the development of time-dependent perturbation theory, it is appropriate to use the interaction picture. In perturbation theory one splits up the Hamiltonian of a system into two parts,

$$\hat{H}(t) = \hat{H}_0 + \hat{\phi}(t) \ , \tag{2.10}$$

where the system described by the unperturbed Hamiltonian $\hat{H}_0$, assumed to be time-independent in all our considerations, is exactly solvable and the perturbative potential $\hat{\phi}(t)$ represents the remaining part of the full Hamiltonian. The operators and states in the interaction picture are both time-dependent, in contrast to the Schrödinger and Heisenberg pictures, and are defined by

$$\hat{O}_D(t) \equiv e^{i\hat{H}_0 t}\hat{O}_S e^{-i\hat{H}_0 t} \ , \ \ |\Psi(t)\rangle_D \equiv e^{i\hat{H}_0 t}|\Psi(t)\rangle_S \ , \tag{2.11}$$

where D labels the interaction (Dirac) picture. The unperturbed Hamiltonian and perturbative potential govern the time-dependence of the operators and states, respectively. In the interaction picture, the time-evolution operator can be written in the form,

$$\hat{U}_D(t,t') = T\exp\left[-i\int_{t'}^{t} d\tau \hat{\phi}_D(\tau)\right] \ , \tag{2.12}$$

for a derivation see [26]. The time-ordering operator T rearranges the operators from left to right with decreasing time-coordinate and with an additional sign change for the interchange of fermionic operators.

Adiabatic Connection

An assumption related to the interaction picture is the *adiabatic connection*. The adiabatic connection of a non-interacting ground state to an interacting ground state was first introduced by Gell-Mann and Low in [27]. It is one of the most important concepts in the current thesis, motivating our choice of approach for constructing the proposed ensemble Green's function formalism for systems of degenerate ground states. In constrast to

this thesis, the adiabatic connection is usually assumed in the development of the zero-temperature Green's function theory for non-degenerate ground states. For a brief review of the concept, see for example [26].

In the adiabatic connection, one assumes that at $t = -\infty$ the interaction is turned off and that the ground state is given by $|\phi_0\rangle$, the lowest energy eigenstate of $\hat{H}_0$. A connection to the interacting ground state $|\Psi(0)\rangle$ at $t = 0$ is established by infinitely slowly turning on the interaction, i.e. adiabatically switching on the interaction. The relation is given by:

$$|\Psi(0)\rangle = \hat{U}_D(0, -\infty)|\phi_0\rangle. \tag{2.13}$$

At $t = +\infty$ the interaction is again assumed to be turned off and one assumes that the state is equal to $|\phi_0\rangle$ with a possible additional phase factor e^{iL}. A second connection to the interacting ground state $|\Psi(0)\rangle$ at $t = 0$ is established by adiabatically switching off the interaction, thus giving the relation:

$$e^{iL}|\phi_0\rangle = \hat{U}_D(+\infty, 0)|\Psi(0)\rangle. \tag{2.14}$$

The main conclusion of the adiabatic connection can now be derived from Eqs. (2.13) and (2.14):

$$e^{iL} = \langle\phi_0|\hat{S}|\phi_0\rangle, \tag{2.15}$$

where $\hat{S}$ is defined as

$$\hat{S} \equiv \hat{U}_D(+\infty, -\infty). \tag{2.16}$$

A consequence of the adiabatic approximation is the following relation,

$$\langle\phi_0|\hat{U}_D(-\infty, 0) = \frac{\langle\phi_0|\hat{U}_D(+\infty, 0)}{\langle\phi_0|\hat{S}|\phi_0\rangle}. \tag{2.17}$$

For a derivation of Eq. (2.17) see for example Ref. [26]. The relation (2.17) is commonly used in the development of the Green's function from the Heisenberg picture to the interaction picture. Notice that the derivation was done for a non-degenerate non-interacting ground state, and that an adiabatic connection between a non-interacting degenerate ground state and an interacting ground state is not clear. The assumption that the state at $t = +\infty$ is equal to the ground state $|\phi_0\rangle$ at $t = -\infty$ with an additional phase factor is not anymore a satisfactory assumption when the non-interacting ground state is degenerate.

2.4 Linear response theory

Linear response theory is a general theory for treating the response of a system to a weak external perturbation. Here, the external perturbation can have many origins, with one possibility being an external electromagnetic field. The main purpose of the current section is to derive the *Kubo formula* and introduce the *linear density response function*. The latter will appear in the Green's function theory approach. For literature on the subject, see for example [28].

The response of a system to an external field is quantified by the change of the ground state expectation value of an operator $\hat{O}(t)$ with the application of an external field $\hat{\phi}(t)$. In linear response theory, the change of the expectation value is computed only to linear order in the external field, assuming the external perturbation to be weak. As an external

field is applied, it is convenient to work in the interaction picture. The time-evolution operator, given by Eq. (2.12), is to first order in the applied field given by:

$$\hat{U}_D(t,0) \approx 1 - i\int_0^t d\tau \hat{\phi}_D(\tau) \ . \tag{2.18}$$

The change in the ground state expectation value of an operator with the application of an external field can now be written in the interaction picture as:

$$\begin{aligned}\delta O(t) &= \langle\Psi_D(t)|\hat{O}_D(t)|\Psi_D(t)\rangle - \langle\Psi_D(0)|\hat{O}_D(t)|\Psi_D(0)\rangle \\ &= \langle\Psi_D(0)|\hat{U}_D(0,t)\hat{O}_D(t)\hat{U}_D(t,0)|\Psi_D(0)\rangle - \langle\Psi_D(0)|\hat{O}_D(t)|\Psi_D(0)\rangle \\ &\approx i\int_0^t dt'\langle\Psi_D(0)|[\hat{\phi}_D(t'),\hat{O}_D(t)]|\Psi_D(0)\rangle. \end{aligned} \tag{2.19}$$

This relation is called the Kubo formula. It should be noticed that a non-degenerate ground state has been assumed. Extensions to the Kubo formula to more general ensemble expectation values will be used in later sections, for both the finite-temperature and ensemble Green's function formalisms.

We now specialize to the case of an external field coupling to the density,

$$\hat{\phi}(t) = \int d^3r\hat{\rho}(r,t)\varphi(r,t), \tag{2.20}$$

describing for example an external electric field. The change in the ground state density can be written as

$$\delta\rho(rt) = i\int d^3r'\int_0^t dt'\varphi(r't')\langle\Psi_D(0)|[\hat{\rho}_D(r't'),\hat{\rho}_D(rt)]|\Psi_D(0)\rangle. \tag{2.21}$$

The *retarded* linear density response function R^r is now defined by

$$\delta\rho(rt) = \int d^3r'\int_0^\infty dt' R^r(rt,r't')\varphi(r't'). \tag{2.22}$$

It describes the density change of the system with respect to the field to linear order in the external field. Comparing Eqs. (2.21) and (2.22), the retarded linear density response function can be identified to be of the form:

$$iR^r(rt,r't') = \langle\Psi_H|[\hat{\rho}_H(rt),\hat{\rho}_H(r't')]|\Psi_H\rangle\theta(t-t'), \tag{2.23}$$

where $\theta(t-t')$ is the Heaviside step function. A common rewritten form of the retarded linear density response function is

$$iR^r(rt,r't') = \langle\Psi_H|[\Delta\hat{\rho}_H(rt),\Delta\hat{\rho}_H(r't')]|\Psi_H\rangle\theta(t-t'), \tag{2.24}$$

where $\Delta\hat{\rho}$ has been introduced:

$$\Delta\hat{\rho}(rt) = \hat{\rho}(rt) - \langle\hat{\rho}(rt)\rangle, \tag{2.25}$$

with the ground state expection value of the density $\langle\hat{\rho}\rangle$.

In the current thesis, the computational approach is based on the computation of time-ordered functions. It is thus convenient to define a *time-ordered* density response function R related to the retarded one. They are related by two simple relations in the

spectral representation. For a time-independent Hamiltonian, the time-dependence of the retarded and time-ordered response functions enters as $\tau = t - t'$. The Fourier transform and inverse Fourier transform are defined as

$$R^r(r, r'; \omega) = \int_{-\infty}^{\infty} d\tau e^{i\omega\tau} R^r(r, r'; \tau) \ , \tag{2.26}$$

$$R^r(r, r'; \tau) = \frac{1}{2\pi} \int_{-\infty}^{\infty} d\omega e^{-i\omega\tau} R^r(r, r'; \omega) \ . \tag{2.27}$$

The spectral represention of the retarded and time-ordered response functions are related by:

$$\mathrm{Re}R(r, r'; \omega) = \mathrm{Re}R^r(r, r'; \omega), \tag{2.28}$$

$$\mathrm{Im}R(r, r'; \omega)\mathrm{sgn}(\omega) = \mathrm{Im}R^r(r, r'; \omega), \tag{2.29}$$

where sgn is the sign-function [28]. The linear density response function which satisfies the relations (2.28) and (2.29) is the following one:

$$iR(rt, r't') = \langle \Psi_H | T\{\Delta\hat{\rho}_H(rt)\Delta\hat{\rho}_H(r't')\} | \Psi_H \rangle. \tag{2.30}$$

In the Green's function theory to be developed, the linear response function will make frequent appearence. By using relations (2.28) and (2.29), the retarded linear response function of physical relevance can then be computed.

2.5 Zero-temperature Green's function theory

The Green's function theory approach is based on the *Green's function* of a many-electron system, which contains physically significant information about the described system. A large library of literature and reviews have been written on the subject, see for example [26, 29].

An intuitive illustration of the Green's function is found in the *PhotoEmission Spectroscopy* (PES) (see figure 2.1) and *Inverse PhotoEmission Spectroscopy* (IPES) experiments. In PES one probes a solid with photons of an energy ω high enough to knock out electrons with momenta $\vec{k}$. A simple view of the energetics is given by,

$$\omega = K + E_B(\vec{k}), \tag{2.31}$$

where K is the kinetic energy of the photo-emitted electron and E_B is the excitation spectrum with the presence of a hole (occupied density of states). Measuring the kinetic energy and momentum of the photo-emitted electrons, one can obtain the excitation spectrum of the solid. Instead, in IPES one probes a solid with electrons, producing the inverse process of PES. One can then measure the excitation spectrum with the presence of an additional electron (unoccupied density of states). The excitation spectra in both experiments are related to the *electron Green's function* in the *sudden* approximation, which corresponds to the limit of large kinetic energy. For an electronic system with a normalized non-degenerate ground state $|\Psi_0\rangle$, the zero-temperature electron Green's function is defined in the Heisenberg picture as

$$G(1, 2) \equiv -i\langle \Psi_0 | T[\hat{\psi}(1)\hat{\psi}^\dagger(2)] | \Psi_0 \rangle, \tag{2.32}$$

where for notational simplicity (r_1, t_1) is written as 1, etc. For $t_1 < t_2$ and $t_1 > t_2$ the physical interpretation of the Green's function is as the probability amplitude for the creation of a hole at r_1 at time t_1 propagating to r_2 at time t_2 and the creation of an electron at r_2 at time t_2 propagating to r_1 at time t_1, respectively. The physical interpretation gives a natural connection to PES and IPES. For $t_1 < t_2$ the Green's function describes the PES experiment, and for $t_1 > t_2$ it describes the IPES experiment.

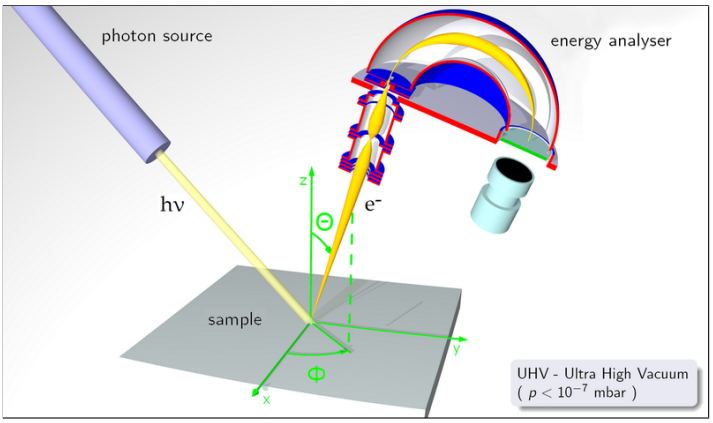

Figure 2.1: Illustration of an *Angle-Resolved PhotoEmission Spectroscopy* (ARPES) experiment. A photon source of an energy $h\nu$ probes a sample, leading to the emission of electrons with kinetic energy measured by an energy analyser at varying angles. Figure taken from [30].

Properties of the electron Green's function will now be detailed. The expectation value of any one-electron operator in the ground state is given by the Green's function as

$$\begin{aligned}\langle\Psi_0|\hat{O}(t)|\Psi_0\rangle &= \int drO(r,t)\langle\Psi_0|\hat{\psi}^\dagger(r,t)\hat{\psi}(r,t)|\Psi_0\rangle \\ &= -i\int drO(r,t)G(rt,rt^+)\ ,\end{aligned} \tag{2.33}$$

where $t^+ = \lim_{\epsilon\to 0^+} t+\epsilon$. As an example, consider Eq. (2.33) in the case of the density operator $\hat{\rho}(r)$:

$$\rho(1) = \langle\Psi_0|\hat{\rho}(1)|\Psi_0\rangle = \langle\Psi_0|\hat{\psi}^\dagger(1)\hat{\psi}(1)|\Psi_0\rangle = -iG(1,1^+), \tag{2.34}$$

with 1^+ corresponding to (r_1, t_1^+). The relation in Eq. (2.34) will be of importance in later derivations. The ground state energy E_0 of a system can be computed from the Green's function by the Galitskii-Migdal formula, given by

$$E_0 = -\frac{i}{2}\int dr \lim_{t'\to t^+}\lim_{r'\to r}\left(i\frac{\partial}{\partial t} + h_0(r)\right)G(rt,r't'), \tag{2.35}$$

for a derivation see for example [28]. The poles of the Fourier transformed Green's function are equal to the exact one-electron excitation energies, also called the exact quasiparticle energies. Quasi-particle in our current considerations specify dressed electrons and holes, affected by the screening of their environment which they interact with. A time-independent Hamiltonian is considered and in this special case the time-dependence of the Green's function enters as $\tau = t - t'$, as for the response functions in section 2.4.

The described pole structure is observed in the following rewritten form of the Green's function, using the Fourier transform defined in Eq. (2.26):

$$G(r_1, r_2; \omega) = \sum_n \frac{\langle \Psi_0^N | \hat{\psi}^\dagger(r_2) | \Psi_n^{N-1} \rangle \langle \Psi_n^{N-1} | \hat{\psi}(r_1) | \Psi_0^N \rangle}{\omega + E_n^{N-1} - E_0^N - i\delta} + \sum_n \frac{\langle \Psi_0^N | \hat{\psi}(r_1) | \Psi_n^{N+1} \rangle \langle \Psi_n^{N+1} | \hat{\psi}^\dagger(r_2) | \Psi_0^N \rangle}{\omega - E_n^{N+1} + E_0^N + i\delta}, \tag{2.36}$$

where E_n^N is the energy of the state $|\psi_n^N\rangle$ for the system with N electrons and δ is an infinitesimal positive constant. For a derivation of Eq. (2.36) see Appendix A. Thus the information contained within the Green's function is the following:

- The expection value of any one-electron operator in the ground state.
- The ground state energy, given by the Galitskii-Migdal formula.
- The one-electron excitation spectrum corresponding to knocking out an electron or adding an additional one.

One is often interested in the *spectral function*, which contains information of, for instance, the *chemical potential* and the density of states. The definition of the spectral function is the following:

$$A(r_1, r_2; \omega) \equiv -\frac{i}{2\pi} \left[G^R(r_1, r_2; \omega) - G^A(r_1, r_2; \omega) \right], \tag{2.37}$$

where $G^R(1,2)$ and $G^A(1,2)$ is the retarded and advanced Green's function, respectively, defined by:

$$G^R(1,2) \equiv -i\Theta(t_1 - t_2) \left(\langle \Psi_0 | \hat{\psi}(1) \hat{\psi}^\dagger(2) | \Psi_0 \rangle + \langle \Psi_0 | \hat{\psi}(2) \hat{\psi}^\dagger(1) | \Psi_0 \rangle \right), \tag{2.38}$$

$$G^A(1,2) \equiv i\Theta(t_2 - t_1) \left(\langle \Psi_0 | \hat{\psi}(1) \hat{\psi}^\dagger(2) | \Psi_0 \rangle + \langle \Psi_0 | \hat{\psi}(2) \hat{\psi}^\dagger(1) | \Psi_0 \rangle \right). \tag{2.39}$$

The Green's function G specifies in our considerations the *time-ordered Green's function*. The Green's function in the case of a non-degenerate ground state can directly be related to the spectral function by the following relations

$$A(1,2;\omega) = -\frac{1}{\pi} \mathrm{sgn}(\omega - \mu) \mathrm{Im} G(1,2;\omega), \tag{2.40}$$

$$G(1,2;\omega) = \int_{-\infty}^{\mu} d\omega' \frac{A(1,2;\omega')}{\omega - \omega' - i\delta} + \int_{\mu}^{\infty} d\omega' \frac{A(1,2;\omega')}{\omega - \omega' + i\delta}, \tag{2.41}$$

with the chemical potential $\mu = E_0^{N+1} - E_0^N$ (called *electron affinity* for finite systems). The trace of the spectral function, defined as

$$Tr[A(\omega)] = \int d1 A(1,1;\omega), \tag{2.42}$$

satisfies a sum rule given by:

$$N = \int_{-\infty}^{\mu} d\omega Tr[A(\omega)], \tag{2.43}$$

where N is the number of electrons in the system. In the beginning of the current section the Green's function was stated to be related to the PES and IPES experiments. A more direct relation exists between the measured excitation spectra in the PES and IPES experiments and the spectral function, with the function being equal to the occupied and unoccupied density of states for $\omega < \mu$ and $\omega > \mu$, respectively.

2.5.1 Equation of motion

The exact Green's function contains important properties and information describing a many-electron system. However, computing the Green's function in the exact case using Eq. (2.36) becomes unfeasible for large and realistic systems. A suitable scheme to compute the Green's function in an approximate way is thus sought. The current and the two following subsections will review the development of such a computational scheme, starting with the development of an equation of motion for the Green's function and an introduction of the *self-energy*, following an approach given in [29].

An equation of motion for the Green's function can be written incorporating the self-energy, a non-local and energy-dependent potential experienced by an electron in a many-electron system. This potential corresponds to the portion of the potential felt by an electron from its surrounding medium originating from its own interaction with that medium. An equation of motion for the Green's function can be constructed from Heisenberg's equation of motion as follows,

$$\left(i\frac{\partial}{\partial t_1} - h_0(1)\right) G(1,2) + i\int d3\; v(1-3)G(1,2,3,3^+) = \delta(1-2), \tag{2.44}$$

with the two-particle Green's function in the Heisenberg picture defined as

$$G^{(2)}(1,2,3,4) \equiv -\langle\Psi_0|T[\hat{\psi}_D(1)\hat{\psi}_D^\dagger(2)\hat{\psi}_D(3)\hat{\psi}_D^\dagger(4)]|\Psi_0\rangle, \tag{2.45}$$

and with the interaction $v(1-2)$ defined as:

$$v(1-2) = v(r_1 - r_2)\delta(t_1 - t_2). \tag{2.46}$$

For a derivation of Eq. (2.44) from Heisenberg's equation of motion see for example [31]. We will use the Schwinger functional derivative technique to further develop the equation of motion and introduce the self-energy. The approach is based on the functional concept, for a short review see Appendix B. In the technique, one introduces a probing field $\varphi(r,t)$, which is set to zero at the end, to express two-particle functions in terms of one-particle functions and their functional derivatives. As a probing field is introduced, it is preferable to work in the interaction picture. The perturbative potential is assumed to be of the form (2.20).

In the interaction picture the one-particle and two-particle electron Green's function are defined as

$$iG(1,2) \equiv \frac{\langle\Psi_0|T[\hat{S}\hat{\Psi}_D(1)\hat{\Psi}_D^\dagger(2)]|\Psi_0\rangle}{\langle\Psi_0|\hat{S}|\Psi_0\rangle}, \tag{2.47}$$

$$G^{(2)}(1,2,3,4) \equiv -\frac{\langle\Psi_0|T[\hat{S}\hat{\Psi}_D(1)\hat{\Psi}_D^\dagger(2)\hat{\Psi}_D(3)\hat{\Psi}_D^\dagger(4)]|\Psi_0\rangle}{\langle\Psi_0|\hat{S}|\Psi_0\rangle}, \tag{2.48}$$

respectively, where $\hat{S}$ is defined by Eq. (2.16). The interaction picture form of the Green's function can be shown to be equivalent to the Heisenberg picture form by the assumption of an adiabatic connection. No assumption of an adiabatic connection will however be required in the current derivations based on the Schwinger functional derivative technique. Notice that the one-particle and two-particle Green's function in the interaction picture return to the Heisenberg picture form in the limit of a vanishing perturbing field ($\hat{S} \to 1$), as required. The dependence of the perturbing field is entirely contained within the $\hat{S}$

operator in the one- and two-electron Green's function. Taking the functional derivative of $\hat{S}$ one obtains:

$$\frac{\delta \hat{S}}{\delta \varphi(3)} = -iT[\hat{S}\hat{\rho}(3)]. \tag{2.49}$$

By the chain-rule for functional derivatives one can derive by using Eqs. (2.34) and (2.49):

$$\frac{\delta G(1,2)}{\delta \varphi(3)} = iG(1,2)\rho(3) - G^{(2)}(1,2,3,3^+). \tag{2.50}$$

Thus the two-particle electron Green's function can be rewritten in terms of the one-particle Green's function and its functional derivative, illustrating the technique.

A problem with the equation of motion (Eq. (2.44)) is the dependence on the two-particle Green's function. An equation of motion of the two-particle Green's function is in turn dependent on the three-particle Green's function etc., leading to a hierarchical problem. To solve this, a common approach is the introduction of a *mass operator*. We now introduce the mass operator M as

$$\begin{aligned} i\int d3\; v(1-3)G(1,2,3,3^+) &\equiv -\int d3\; M(1,3)G(3,2), \\ M(1,4) &= -i\int d3d2\; v(1-3)G^{(2)}(1,2,3,3^+)G^{-1}(2,4). \end{aligned} \tag{2.51}$$

By using Eq. (2.50) one can rewrite the mass operator:

$$\begin{aligned} M(1,4) &= -i\int d2d3\; v(1-3)\left[iG(1,2)\rho(3) - \frac{\delta G(1,2)}{\delta \varphi(3)}\right] G^{-1}(2,4) \\ &= V^H(1)\delta(1-4) + \Sigma(1,4), \end{aligned} \tag{2.52}$$

where the Hartree potential V^H and self-energy Σ are introduced as:

$$V^H(1) \equiv \int d3\; v(1-3)\rho(3), \tag{2.53}$$

$$\Sigma(1,2) \equiv -i\int d3d4\; v(1-3)G(1,4)\frac{\delta G^{-1}(4,2)}{\delta \varphi(3)}. \tag{2.54}$$

In Eq. (2.54) the identity

$$\int d2\; \frac{\delta G(1,2)}{\delta \varphi(3)}G^{-1}(2,4) = -\int d2\; G(1,2)\frac{\delta G^{-1}(2,4)}{\delta \varphi(3)}, \tag{2.55}$$

derived from the chain-rule for functional derivatives, has been used. One can now construct the sought form of the equation of motion for the Green's function incorporating the self-energy:

$$\left(i\frac{\partial}{\partial t_1} - h(1)\right)G(1,2) - \int d3\; \Sigma(1,3)G(3,2) = \delta(1-2), \tag{2.56}$$

with $h(1) \equiv h_0(1) + V^H(1) + \varphi(1)$.

The inverse Green's function can with Eq. (2.56) be written in the form

$$G^{-1}(1,2) = \left(i\frac{\partial}{\partial t_1} - h(1)\right)\delta(1-2) - \Sigma(1,2), \tag{2.57}$$

and its functional derivative with respect to the perturbing field is thus given by

$$\frac{\delta G^{-1}(1,2)}{\delta\varphi(3)} = -\left(\delta(1-3) + \frac{\delta V^H(1)}{\delta\varphi(3)}\right)\delta(1-2) - \frac{\delta\Sigma(1,2)}{\delta\varphi(3)}. \tag{2.58}$$

An iterative equation for the self-energy can now be constructed by Eqs. (2.54) and (2.58) as:

$$\begin{aligned}\Sigma(1,4) = iv(1-4)G(1,4) + i\int d3\; v(1-3)G(1,4)\frac{\delta V^H(4)}{\delta\varphi(3)} \\ + i\int d2\,d3\; v(1-3)G(1,2)\frac{\delta\Sigma(2,4)}{\delta\varphi(3)}.\end{aligned} \tag{2.59}$$

An equation of motion for the Green's function incorporating the self-energy (Eq. (2.56)) and an iterative equation for the self-energy (Eq. (2.59)) have thus been derived.

2.5.2 Hedin's equations

A set of equations called *Hedin's equations*, equivalent to the Green's function equation of motion (Eq. (2.56)) and the iterative equation for the self-energy (Eq. (2.59)), can be constructed. It is a set of five self-consistent equations for the Green's function, originally developed by L. Hedin in 1965 [14], and will be the basis for the computational approach considered in this thesis. For more in-depth reviews of Hedin's equations see for example [29, 32].

The first of Hedin's equations is the *Dyson equation*. It relates the Green's function G to the self-energy Σ and the *non-interacting Green's function* G^0. The latter is defined as the Green's function satisfying Eq. (2.56) for $\Sigma(1,2) = 0$. The Dyson equation can be constructed from Eq. (2.56) as:

$$G(r_1, r_2; \omega) = G^0(r_1, r_2; \omega) + \int d3\,d4\; G^0(r_1, r_3; \omega)\Sigma(r_3, r_4; \omega)G(r_4, r_2; \omega). \tag{2.60}$$

The second of Hedin's equations relates the self-energy Σ to the *screened interaction* W and *vertex function* Λ, defined by

$$W(1,2) \equiv \int d3\; v(2-3)\frac{\delta V(1)}{\delta\varphi(3)}, \quad \Lambda(1,2,3) \equiv -\frac{\delta G^{-1}(1,2)}{\delta V(3)}, \tag{2.61}$$

with the total field $V \equiv V^H + \varphi$ introduced. The physical interpretation of W is as the screened Coulomb interaction. By the introduction of W and Λ one can rewrite Eq. (2.54) with the chain-rule for functional derivatives as:

$$\Sigma(1,2) = i\int d4\,d5\; G(1,4)\Lambda(4,2,5)W(5,1). \tag{2.62}$$

The response of a system with respect to an external field is a property of interest in many-electron systems, see section 2.4. A polarization P and response function R are introduced, expressing the response of the electronic system with respect to the total field V and the external field φ, respectively. The two functions can be defined as

$$P(1,2) \equiv \frac{\delta\rho(1)}{\delta V(2)}, \quad R(1,2) \equiv \frac{\delta\rho(1)}{\delta\varphi(2)}. \tag{2.63}$$

Both functions can be related via:

$$R(1,2) = P(1,2) + \int d3\,d4\; P(1,3)v(3-4)R(4,2). \tag{2.64}$$

Often it is enough to consider only the the linear density response function of a many-electron system. In frequency space the linear density response function can be written as:

$$R(r_1,r_2;\omega) = \sum_{n\neq 0}\left[\frac{\langle\Psi_0|\hat{\rho}(r_1)|\Psi_n\rangle\langle\Psi_n|\hat{\rho}(r_2)|\Psi_0\rangle}{\omega - E_n + E_0 + i\delta} - \frac{\langle\Psi_0|\hat{\rho}(r_2)|\Psi_n\rangle\langle\Psi_n|\hat{\rho}(r_1)|\Psi_0\rangle}{\omega + E_n - E_0 - i\delta}\right]. \tag{2.65}$$

See Appendix C for a derivation of Eq. (2.65). The linear response function can be related to the retarded linear response function as described in section 2.4. The spectral form of the response function, defined as:

$$S(r_1,r_2;\omega) = -\frac{1}{\pi}\mathrm{sgn}(\omega)\mathrm{Im}R(r_1,r_2;\omega), \tag{2.66}$$

will be an additional form of the response function used in the current thesis. The third of Hedin's equations, relating the screened interaction W to the polarization P, can be obtained from Eqs. (2.61) and (2.63) as

$$W(1,2) = v(1-2) + \int d3\,d4\; v(1-3)P(3,4)W(4,2), \tag{2.67}$$

where the chain-rule for functional derivatives has been employed.

The fourth of Hedin's equations relates the polarization P to the Green's function G and vertex function Λ. The equation can be obtained by rewriting Eq. (2.63), using the chain-rule for functional derivatives and partial integration, as

$$P(1,2) = -i\int d3\,d4\; G(1,3)\Lambda(3,4,2)G(4,1^+)\;. \tag{2.68}$$

The final Hedin equation is obtained by rewriting Eq. (2.61) as

$$\begin{aligned}\Lambda(1,2,3) &= \delta(1-2)\delta(1-3) + \frac{\delta\Sigma(1,2)}{\delta V(3)} \\ &= \delta(1-2)\delta(1-3) + \int d4\,d5\,d6\,d7\;\frac{\delta\Sigma(1,2)}{\delta G(4,5)}G(4,6)G(7,5)\Lambda(6,7,3),\end{aligned} \tag{2.69}$$

by employing the chain-rule for functional derivatives and partial integration. The Hedin equations are the set of self-consistent Eqs. (2.60), (2.62), (2.67), (2.68) and (2.69) for the computation of the Green's function. It corresponds to an exact set of equations, but approximations and computational schemes are required for practical applications.

2.5.3 *GW* approximation

The *GW-Approximation* (GWA) is an approximation to Hedin's equations, originally proposed by L. Hedin in [14]. The approximation corresponds to the simplest non-trivial approximation to the self-energy beyond the Hartree-Fock approximation. For in-depth

reviews of GWA see for example [29, 32]. In the GWA one sets $\delta\Sigma/\delta V = 0$ in Eq. (2.69), thus approximating the vertex function as

$$\Lambda(1,2,3) = \delta(1-2)\delta(1-3), \tag{2.70}$$

further modifying Eqs. (2.62) and (2.68):

$$\Sigma(1,2) = iG(1,2)W(2,1), \tag{2.71}$$
$$P(1,2) = -iG(1,2)G(2,1^+). \tag{2.72}$$

The form of the self-energy in Eq. (2.71) is the origin of the name for GWA. GWA can be considered a generalization of the Hartree-Fock approximation, with the bare Coulomb interaction v replaced by the screened Coulomb interaction W from electron-hole screening.

Computations within GWA are usually done within the *Random-Phase Approximation* (RPA): an approximation to the linear response function. The linear density response function can using Eqs. (2.34),(2.55),(2.58) and (2.63) be written in the form:

$$R(1,2) = -i\int d3d4\; G(1,3)\left[\delta(3-2)\delta(4-2) + \frac{\delta V^H(3)}{\delta\varphi(2)}\delta(4-2) + \frac{\delta\Sigma(3,4)}{\delta\varphi(2)}\right]G(4,1^+). \tag{2.73}$$

The RPA corresponds to setting $\delta\Sigma/\delta\varphi = 0$, leading to the RPA equation:

$$R(1,2) = P^0(1,2) + \int d3d4\; P^0(1,3)v(3-4)R(4,2). \tag{2.74}$$

The introduced non-interacting polarization P^0 is of the same form as the linear response function, given by Eq. (2.65), with the non-interacting states and energies used instead of the interacting ones. RPA corresponds to assuming that the response of an interacting system to an external field is given by the response of a non-interacting system to the total field. Assuming RPA further modifies Eq. (2.67):

$$W(1,2) = v(1-2) + \int d3d4\; v(1-3)P^0(3,4)W(4,2). \tag{2.75}$$

Two commonly used computational schemes based on the GWA are the one-shot G^0W^0 approach and the iterative self-consistent GW approach. See Fig. 2.2 for a diagrammatic view of the schemes and for more information on the schemes see [29, 32]. The initial step in the G^0W^0 approach is to construct the non-interacting states and energies from a self-consistent mean-field approach. Thereafter, the spin-polarized non-interacting Green's function, corresponding to G^0 separate into each spin channel, and non-interacting polarization, corresponding to the sum over the contributions for each spin channel, are computed. In turn the screened interaction W is computed from P^0. The computation of the spin-polarized self-energy Σ can be separated into an exchange and correlation part. The exchange part is given by:

$$\Sigma^x(r_1, r_2; \omega) = -v(r_1 - r_2)\sum_n^{\text{occ}} \phi_n(r_1)\phi_n^*(r_2), \tag{2.76}$$

setting the Green's function to the non-interacting one. The imaginary part of the correlation self-energy is given by

$$\mathrm{Im}\Sigma^c(r_1, r_2; \omega \leq \mu) = -\sum_n^{\mathrm{occ}} \phi_n(r_1)\phi_n^*(r_2)\mathrm{Im}W^c(r_1, r_2; \epsilon_n - \omega)\theta(\epsilon_n - \omega), \tag{2.77}$$

$$\mathrm{Im}\Sigma^c(r_1, r_2; \omega > \mu) = \sum_n^{\mathrm{unocc}} \phi_n(r_1)\phi_n^*(r_2)\mathrm{Im}W^c(r_1, r_2; \omega - \epsilon_n)\theta(\omega - \epsilon_n), \tag{2.78}$$

with non-interacting Green's function used and with the introduction of $W^c \equiv W - v$. Furthermore, the orbital eigenenergies ϵ_n are defined as

$$\epsilon_n = \begin{cases} E_n^{N+1} - E_0^N, & n \text{ occupied}, \\ E_0^N - E_n^{N-1}, & n \text{ unoccupied}. \end{cases} \tag{2.79}$$

Defining the spectral form Γ of the correlation self-energy as

$$\Gamma(r_1, r_2; \omega) = -\frac{1}{\pi}\mathrm{sgn}(\omega - \mu)\mathrm{Im}\Sigma^c(r_1, r_2; \omega), \tag{2.80}$$

one can compute the real part of the correlation self-energy as the Hilbert transform of Γ like the following:

$$\mathrm{Re}\Sigma^c(r_1, r_2; \omega) = P\int_{-\infty}^{\infty} d\omega' \frac{\Gamma(r_1, r_2; \omega')}{\omega - \omega'}, \tag{2.81}$$

with P specifying a principle value integral. The Green's function G is finally computed by the Dyson equation.

The self-consistent GW approach is an iterative approach repeating the same computational structure as the G^0W^0 approach. The procedure is initialized by the G^0W^0 approach and in each iteration the Green's function is updated and used in the iteration that follows.

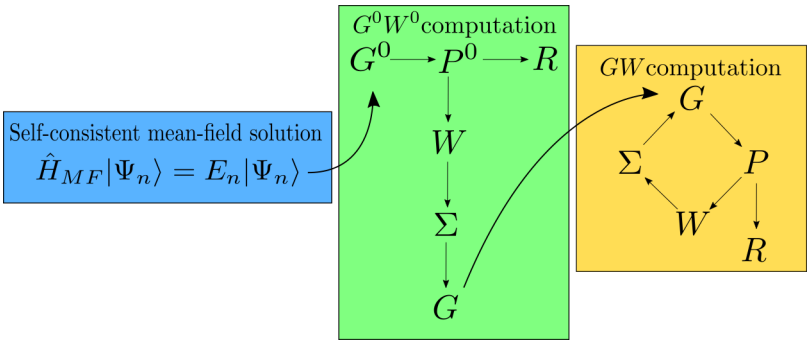

Figure 2.2: Diagrammatic view of the computational scheme used in the G^0W^0 and GW approach. The initial step (left) corresponds to a self-consistent mean-field approach. The first iteration corresponds to the G^0W^0 approach (middle) and the iterative self-consistent approach corresponds to the GW approach (right).

2.6 Finite-temperature Green's function theory

The Green's function theory for finite temperature will be reviewed here. The theory will appear when later compared to our proposed ensemble Green's function theory as

well as when an extension of the finite-temperature formalism to systems with degenerate states is proposed. The inclusion of temperature introduces both complications as well as simplifications relative to the zero-temperature formalism. The computations in the temperature case can be separated into two parts: the treatment of the *Matsubara Green's function* $\mathcal{G}$ and the treatment of the *real-time Green's function* $\bar{G}$. In the current section, non-degenerate states will be assumed. For literature on the subject see for example [28].

For electronic systems at finite temperature it is convenient to work in the *grand canonical ensemble*. The grand canonical ensemble is a statistical ensemble of states of a system in both thermal and chemical thermodynamical equilibrium with a reservoir. The grand partition function and statistical operator are defined by,

$$Z_G \equiv \mathrm{Tr}\left[e^{-\beta\hat{K}}\right], \;\; \hat{\rho}_G \equiv Z_G^{-1} e^{-\beta\hat{K}}, \tag{2.82}$$

where $\beta = (k_B T)^{-1}$, k_B is the Boltzmann constant, T is the temperature of the system and $\hat{K}$ is the modified Hamiltonian, defined by:

$$\hat{K} \equiv \hat{H} - \mu\hat{N}, \tag{2.83}$$

where $\hat{N}$ is the number operator. The trace is over all states of the system. It is convenient to subsequently introduce the *modified* Heisenberg picture as

$$\hat{O}_K(\tau) \equiv e^{\hat{K}\tau}\hat{O}_S e^{-\hat{K}\tau} \;, \;\; |\Psi(\tau)\rangle_S \equiv e^{-\hat{K}\tau}|\Psi\rangle_K \;, \tag{2.84}$$

with K labeling the modified Heisenberg picture. Observe that the field operators in the modified Heisenberg picture are of the form:

$$\hat{\psi}_K(\tau) = e^{\hat{K}\tau}\hat{\psi}_S e^{-\hat{K}\tau} \;, \;\; \hat{\psi}_K^\dagger(\tau) = e^{\hat{K}\tau}\hat{\psi}_S^\dagger e^{-\hat{K}\tau} \;, \tag{2.85}$$

and thus for real τ the two field operators are not adjoint. For the imaginary time $\tau = it$ the two field operators are adjoint however, and this is the convention which will be used. As long as τ is interpreted as a complex variable, it can be treated as purely imaginary by an analytic continuation.

The one-electron Matsubara Green's function $\mathcal{G}$ can now be defined as

$$\mathcal{G}(1,2) \equiv -\mathrm{Tr}\{\hat{\rho}_G T_\tau[\hat{\psi}_K(1)\hat{\psi}_K^\dagger(2)]\}, \tag{2.86}$$

where T_τ is the imaginary time-ordering operator, defined equivalentely to the time-ordering operator, but for imaginary time τ. The Matsubara Green's function contains information required to compute equilibrium thermodynamic properties. The ensemble average expectation value of any one-electron operator, the ensemble average of the Hamiltonian and the thermodynamic potential can be computed directly from $\mathcal{G}$.

As with the zero-temperature formalism, it is appropriate to work in the interaction picture. Splitting up the modified Hamiltonian of a system into two parts,

$$\hat{K}(t) = \hat{K}_0 + \hat{K}_1(t), \tag{2.87}$$

with an unperturbed modified Hamiltonian $\hat{K}_0$ and the remaining part $\hat{K}_1$ of the modified Hamiltonian. The *modified* interaction picture, denoted I, is now defined by:

$$\hat{O}_I(\tau) \equiv e^{\hat{K}_0\tau}\hat{O}_S e^{-\hat{K}_0\tau} \;, \;\; |\Psi(\tau)\rangle_S \equiv e^{-\hat{K}_0\tau}|\Psi(\tau)\rangle_I \;. \tag{2.88}$$

In the modified interaction picture, the imaginary time-evolution operator can be written, similarly to the normal interaction picture, in the form:

$$\hat{\mathcal{U}}(\tau,\tau') = T_\tau \exp\left[-\int_{\tau'}^{\tau} d\tau'' \hat{K}_1(\tau'')\right]. \tag{2.89}$$

The partion function and the imaginary time-evolution operator are related by the following relation:

$$Z_G = \mathrm{Tr}\left[e^{-\beta\hat{K}_0}\hat{\mathcal{U}}(\beta,0)\right]. \tag{2.90}$$

An important feature of this relation is that all the integrals in the imaginary-time evolution operator are over a finite range. The exact Matsubara Green's function can now be written in the modified interaction picture as

$$\mathcal{G}(1,2) = -\frac{\mathrm{Tr}\left\{e^{-\beta\hat{K}_0}T_\tau\left[\hat{\mathcal{U}}(\beta,0)\hat{\psi}_I(1)\hat{\psi}_I^\dagger(2)\right]\right\}}{\mathrm{Tr}\left\{e^{-\beta\hat{K}_0}\hat{\mathcal{U}}(\beta,0)\right\}}. \tag{2.91}$$

Notice that no assumption of adiabatic connection is used in the temperature formalism derivations. This aspect orginates from the finite range in the integration, instead of the infinite range in the zero-temperature scenario, making an assumption of an adiabatic connection irrelevant. The finite range of the integration is in turn related to a fundamental periodicity of the Matsubara Green's function with respect to $\tau - \tau'$ with a period of 2β. The Matsubara Green's function formalism leads to the same set of equations as the zero-temperature Green's function formalism. Thus the Green's function equation of motion and iterative equation for the self-energy are of identical form to the zero-temperature formalism, and the computational scheme for the Matsubara Green's function can be constructed identically to the one for the zero-temperature Green's function.

A property of interest from the zero-temperature Green's function is the quasiparticle energy spectrum. The quasiparticle energies are however not directly related to the poles of the frequency space Matsubara Green's function. To compute the quasiparticle energy spectrum for finite temperature one introduces the real-time Green's function $\bar{G}$, defining it as

$$\bar{G}(1,2) \equiv -i\mathrm{Tr}\{\hat{\rho}_G T[\hat{\psi}_K(1)\hat{\psi}_K^\dagger(2)]\}, \tag{2.92}$$

containing the quasiparticle energy spectrum in the same way as in the zero-temperature case. The real-time Green's function can be computed from the Matsubara Green's function directly by an analytic continuation. The quasiparticle energies can thus be determined without the use of an adiabatic connection.

As for zero-temperature, the retarded linear real-time response function is a property of interest. By the Kubo formula, as in section 2.4, the *retarded real-time linear response function* can be written as:

$$iR^r(1,2) = \mathrm{Tr}\left\{\hat{\rho}_G[\Delta\hat{\rho}_H(rt), \Delta\hat{\rho}_H(r't')]\right\}\theta(t-t'), \tag{2.93}$$

where $\Delta\hat{\rho}$ now is defined

$$\Delta\hat{\rho}(rt) = \hat{\rho}(rt) - \langle\hat{\rho}(rt)\rangle, \tag{2.94}$$

with the ensemble averaged expection value of the density $\langle\hat{\rho}\rangle$. A *time-ordered* real-time linear response function is required to satisfy the relations (2.28) and (2.29), giving it the

form:

$$R(r_1, r_2; \omega) = {Z_G}^{-1} \sum_{n,m} \langle \Psi_n | \Delta\hat{\rho}(r_1) | \Psi_m \rangle \langle \Psi_m | \Delta\hat{\rho}(r_2) | \Psi_n \rangle \times \left[\frac{e^{-\beta K_n}}{\omega - K_m + K_n + i\delta} - \frac{e^{-\beta K_m}}{\omega - K_m + K_n - i\delta} \right], \tag{2.95}$$

with eigenvalues K_n and eigenstates $|\Psi_n\rangle$ of $\hat{K}$. See Appendix C for derivations of Eqs. (2.93) and (2.95). The real-time linear density response function can be related by an analytic continuation to a Matsubara linear density response function $\mathcal{R}$, defined analogously to the Green's function.

Chapter 3

Ensemble Green's function theory

In the current chapter, the proposed ensemble Green's function theory will be introduced, and the formalism developed. Furthermore, a one-shot and a self-consistent computational scheme for the computation of the ensemble Green's function is constructed within the ensemble analogue of GWA. The chapter ends with a comparison between the ensemble and temperature formalisms in the limit of $T \to 0^+$, and an extension of the finite-temperature formalism to systems including degenerate states is proposed.

3.1 Ensemble Green's function

We propose an ensemble Green's function formalism for systems of interacting electrons with degenerate ground states based on the von Neumann density matrix formalism. An ensemble Green's function is defined similar to the ensemble density, see Eq. (2.7) in section 2.2, as

$$G(1,2) \equiv \sum_{n=1}^{M} w_n G_n(1,2), \quad \sum_{i=1}^{M} w_i = 1, \quad 0 \leq w_i \leq 1, \tag{3.1}$$

with $G_n(1,2)$ defined in the interaction picture by

$$iG_n(1,2) = \frac{\langle \Psi_n | T[\hat{S}\hat{\psi}_D(1)\hat{\psi}_D^\dagger(2)] | \Psi_n \rangle}{\langle \Psi_n | \hat{S} | \Psi_n \rangle}, \tag{3.2}$$

for a system prepared in the ensemble of states $\{|\Psi_n\rangle, n = 1, ..., M\}$ with corresponding fractions w_n at an initial time. The perturbative potential is defined by Eq. (2.20). The set $\{|\Psi_n\rangle, n = 1, ..., M\}$ is a set of arbitrary many-electron states, and will later be chosen as the degenerate interacting ground states with uniform weights. Different definitions for the denominator of Eq. (3.2) can be imagined and a motivation for the choice of denominator will therefore be expanded upon in subsections 3.1.2 and 3.1.4. Notice that no assumption of an adiabatic connection is made in the definition of the ensemble Green's function. The ambiguous connection between a true interacting ground state and a non-interacting degenerate ground state, as mentioned previously in section 2.3, is avoided.

As in the non-degenerate case, the ensemble Green's function contains physically significant information of the described many-electron system. The ensemble expectation

value of any one-particle operator can be obtained from the ensemble Green's function as

$$\begin{aligned}\left\langle \hat{O} \right\rangle &\equiv \sum_{n=1}^{m} w_n \left\langle \Psi_n | \hat{O} | \Psi_n \right\rangle \\ &= -i \int dr \lim_{r' \to r} O(r) G(rt, r't^+), \end{aligned} \tag{3.3}$$

which is of the same form as in the non-degenerate case (Eq. (2.33)) except that the ensemble Green's function is used instead. The set $\{|\Psi_n\rangle, n = 1, ..., M\}$ will now momentarily be chosen as the set of degenerate interacting ground states with uniform weights $w_i = 1/M$. The Galitskii-Migdal formula in the ensemble case is derived to be of an identical form to the non-degenerate case, except with the ensemble Green's function used instead,

$$E_0 = -\frac{i}{2} \int dr \lim_{t' \to t^+} \lim_{r' \to r} \left(i\frac{\partial}{\partial t} + h_0(r) \right) G(rt, r't'). \tag{3.4}$$

Additionally, the ensemble Green's function can be written in the form:

$$\begin{aligned} G(1,2;\omega) = &\frac{1}{M} \sum_{n=1}^{M} \sum_{m} \frac{\langle \Psi_n^N | \hat{\psi}^\dagger(2) | \Psi_m^{N-1} \rangle \langle \Psi_m^{N-1} | \hat{\psi}(1) | \Psi_n^N \rangle}{\omega + E_m^{N-1} - E_0^N - i\delta} \\ &+ \frac{1}{M} \sum_{n=1}^{M} \sum_{m} \frac{\langle \Psi_n^N | \hat{\psi}(1) | \Psi_m^{N+1} \rangle \langle \Psi_m^{N+1} | \hat{\psi}^\dagger(2) | \Psi_n^N \rangle}{\omega - E_m^{N+1} + E_0^N + i\delta}, \end{aligned} \tag{3.5}$$

with the poles, i.e. $\omega = \pm(E_m^{N\pm1} - E_0^N)$, being as in the non-degenerate case equal to the exact quasiparticle energies. Thus the information contained within the ensemble Green's function is the following:

- The ensemble expection value of any one-electron operator in the degenerate ground state ensemble.
- The ensemble average of the ground state energy, by the ensemble version of the Galitskii-Migdal formula.
- The one-electron excitation spectrum corresponding to knocking out an electron or adding an additional one.

The set $\{|\Psi_n\rangle, n = 1, ..., M\}$ will now for the remainder of the development of the formalism correspond to an arbitrary set of many-electron states, unless otherwise specified.

3.1.1 Equation of motion

As in the non-degenerate case, an equation of motion for the Green's function G_n and a corresponding self-energy Σ_n can be introduced in the ensemble case. The G_n Green's functions are of the same form as a non-degenerate Green's function, and thus satisfy the set of equations of motion:

$$\left(i\frac{\partial}{\partial t_1} - h_0(1) \right) G_n(1,2) + i \int d3\, v(1-3) G_n^{(2)}(1,2,3,3^+) = \delta(1-2), \tag{3.6}$$

with the two-particle Green's functions $G_n^{(2)}$ defined in the interaction picture as:

$$G_n^{(2)}(1,2,3,4) = -\frac{\left\langle \Psi_n | T[\hat{S}\hat{\psi}_D(1)\hat{\psi}_D^\dagger(2)\hat{\psi}_D(3)\hat{\psi}_D^\dagger(4)] | \Psi_n \right\rangle}{\left\langle \Psi_n | \hat{S} | \Psi_n \right\rangle}. \tag{3.7}$$

The Schwinger functional derivative technique will now be utilized. By the chain-rule for functional derivatives one obtains

$$\frac{\delta G_n(1,2)}{\delta\varphi(3)} = iG_n(1,2)\rho_n(3) - G_n^{(2)}(1,2,3,3^+) \tag{3.8}$$

where the density ρ_n is given by:

$$\rho_n(1) = \langle \Psi_n | \hat{\rho}(1) | \Psi_n \rangle = -iG_n(1,1^+). \tag{3.9}$$

We now introduce the mass operators $M_n(1,2)$ as

$$\begin{aligned} i\int d3\; v(1-3)G_n(1,2,3,3^+) &= -\int d3\; M_n(1,3)G_n(3,2), \\ M_n(1,4) &= -i\int d2d3\; v(1-3)G_n^{(2)}(1,2,3,3^+)G_n^{-1}(2,4). \end{aligned} \tag{3.10}$$

By using Eq. (3.8) one can further rewrite the mass operator as

$$\begin{aligned} M_n(1,4) &= -i\int d2d3\; v(1-3)\left[iG_n(1,2)\rho_n(3) - \frac{\delta G_n(1,2)}{\delta\varphi(3)}\right] G_n^{-1}(2,4) \\ &= V^H(1)\delta(1-4) + \Sigma_n(1,4), \end{aligned} \tag{3.11}$$

where we have introduced the ensemble Hartree potential V^H and self-energies Σ_n as

$$V^H(1) \equiv \sum_{n=1}^{M} w_n V_n^H(1) \equiv \sum_{n=1}^{M} w_n \int d3\; v(1-3)\rho_n(3), \tag{3.12}$$

$$\Sigma_n(1,2) \equiv -i\int d3d4\; v(1-3)G_n(1,4)\frac{\delta G_n^{-1}(4,2)}{\delta\varphi(3)} + \delta(1-2)\left(V_n^H(1) - V^H(1)\right). \tag{3.13}$$

The ensemble Hartree potential V^H is treated instead of the separate Hartree potentials V_n^H, thus modifying the self-energy. The choice is motivated by the fact that in the degenerate case, the self-consistent mean-field Hamiltonian approach is in general only well-defined for an ensemble mean-field Hamiltonian. The concept of degeneracy becomes ill-defined when using separate Hartree potentials V_n^H as the degeneracy as perceived by two different degenerate ground states may differ, and thus an issue arises in which states to treat as degenerate ground states. The equation of motion for G_n can now be written, using the introduced Σ_n, as:

$$\left(i\frac{\partial}{\partial t_1} - h(1)\right) G_n(1,2) - \int d3\; \Sigma_n(1,3)G_n(3,2) = \delta(1-2), \tag{3.14}$$

with $h(1) \equiv h_0(1) + V^H(1) + \varphi(1)$.

The inverse Green's function G_n is obtained from Eq. (3.14) as

$$G_n^{-1}(4,2) = \left(i\frac{\partial}{\partial t_4} - h(4)\right)\delta(4-2) - \Sigma_n(4,2), \tag{3.15}$$

and its functional derivative with respect to the probing field thus becomes:

$$\frac{\delta G_n^{-1}(4,2)}{\delta\varphi(3)} = -\left(\delta(4-3) + \frac{\delta V^H(4)}{\delta\varphi(3)}\right)\delta(4-2) - \frac{\delta\Sigma_n(4,2)}{\delta\varphi(3)}. \tag{3.16}$$

An iterative equation for the self-energy is now obtained as

$$\begin{aligned}\Sigma_n(1,2) = iG_n(1,2)v(1-2) &+ i\int d3\; v(1-3)G_n(1,2)\frac{\delta V^H(2)}{\delta\varphi(3)} \\ &+ i\int d3d4\; v(1-3)G_n(1,4)\frac{\delta\Sigma_n(4,2)}{\delta\varphi(3)} \\ &+ \delta(1-2)\left(V_n^H(1) - V^H(1)\right),\end{aligned} \tag{3.17}$$

which is of the same form as in the non-degenerate case (Eq. (2.59)) except for the modification of the Hartree term.

An equation of motion for G_n (Eq. (3.14)) and an iterative equation for the self-energy Σ_n (Eq. (3.17)) have thus been constructed. The proposed approach is based on auxiliary functions G_n and Σ_n, instead of an ensemble Green's function G and an *ensemble* self-energy Σ. The motivation for this approach will now be discussed. An equation of motion for G can be constructed by multiplying both sides of Eq. (3.14) with w_n and summing over n:

$$\left(i\frac{\partial}{\partial t_1} - h(1)\right)G(1,2) - \int d3\;\Sigma(1,3)G(3,2) = \delta(1-2), \tag{3.18}$$

where the ensemble self-energy is introduced:

$$\Sigma(1,4) \equiv \sum_{n=1}^{M} w_n \int d2d3\;\Sigma_n(1,3)G_n(3,2)G^{-1}(2,4). \tag{3.19}$$

An iterative equation for the self-energy can be derived to be of the form:

$$\begin{aligned}\Sigma(1,2) = iG(1,2)v(1-2) &+ i\int d3\; v(1-3)G(1,2)\frac{\delta V^H(2)}{\delta\varphi(3)} \\ &+ i\int d3d4\; v(1-3)G(1,4)\frac{\delta\Sigma(4,2)}{\delta\varphi(3)} \\ &+ \sum_{n=1}^{M}\int d3 w_n G_n(1,3)G^{-1}(3,2)\left(V_n^H(1) - V^H(1)\right).\end{aligned} \tag{3.20}$$

The dependence on G_n in the iterative equation (3.20) poses a problem. As G does not contain all the information required to compute the separate G_n, a self-consistent approach is not possible by working only with G and Σ. By working with the auxiliary functions G_n and Σ_n, this problem does not arise, thus motivating the choice of approach. This is natural, as the information of the ensemble is required to be contained within the self-consistent computation.

3.1.2 Ensemble Hedin's equations

An ensemble analogue of the Hedin's equations can now be derived as a set of five self-consistent equations for the ensemble Green's function. We now further specify the

$\{|\Psi_n\rangle, n = 1, ..., M\}$ as the set of degenerate interacting ground states with a degeneracy M and with equal weights $w_n = 1/M$.

The first ensemble Hedin equation is a set of Dyson equations. By the introduction of the non-interacting Green's functions G_n^0, defined to satisfy Eq. (3.14) for $\Sigma_n(1,2) = 0$, the set of Dyson equations can be written as:

$$G_n(r_1, r_2; \omega) = G_n^0(r_1, r_2; \omega) + \int d3\, d4\; G_n^0(r_1, r_3; \omega)\Sigma_n(r_3, r_4; \omega)G_n(r_4, r_2; \omega). \tag{3.21}$$

The second ensemble Hedin equation relates the self-energies Σ_n to the ensemble screened interaction W and vertex functions Λ_n, defined by

$$W(1,2) \equiv \int d3\; v(2-3)\frac{\delta V(1)}{\delta\varphi(3)}, \quad \Lambda_n(1,2,3) \equiv -\frac{\delta G_n^{-1}(1,2)}{\delta V(3)}, \tag{3.22}$$

with the introduction of the total field $V = V^H + \varphi$. By introducing W and Λ_n, one can rewrite Eq. (3.13) with the chain-rule for functional derivatives as the second ensemble Hedin's equation:

$$\Sigma_n(1,2) = i\int d4\, d5\; G_n(1,4)\Lambda_n(4,2,5)W(5,1) + \delta(1-2)\left(V_n^H(1) - V^H(1)\right). \tag{3.23}$$

An ensemble polarization P and ensemble response function R can be defined as

$$P(1,2) \equiv \frac{\delta\rho(1)}{\delta V(2)} = \frac{1}{M}\sum_{n=1}^{M}\frac{\delta\rho_n(1)}{\delta V(2)} \equiv \frac{1}{M}\sum_{n=1}^{M} P_n(1,2), \tag{3.24}$$

$$R(1,2) \equiv \frac{\delta\rho(1)}{\delta\varphi(2)} = \frac{1}{M}\sum_{n=1}^{M}\frac{\delta\rho_n(1)}{\delta\varphi(2)} \equiv \frac{1}{M}\sum_{n=1}^{M} R_n(1,2), \tag{3.25}$$

where the P and R are related to the separate polarizations P_n and response functions R_n. As in the non-degenerate case, the relation between the two functions can be written in the form:

$$R(1,2) = P(1,2) + \int d3\, d4\; P(1,3)v(3-4)R(4,2). \tag{3.26}$$

A third ensemble Hedin equation, relating the ensemble screened interaction W to the polarization P, can by Eq. (3.22) and the chain-rule for functional derivatives be derived as:

$$W(1,2) = v(1-2) + \int d3\, d4\; v(1-3)P(3,4)W(4,2). \tag{3.27}$$

A property of interest for many-electron systems, as stated in section 2.5, is the linear response function. In frequency space the linear ensemble density response function can be written as:

$$\begin{aligned} R(r_1, r_2; \omega) &\equiv \frac{1}{M}\sum_{n=1}^{M} R_n(r_1, r_2; \omega) \\ &= \frac{1}{M}\sum_{n=1}^{M}\sum_{m\neq n}\left[\frac{\langle\Psi_n|\hat{\rho}(r_1)|\Psi_m\rangle\langle\Psi_m|\hat{\rho}(r_2)|\Psi_n\rangle}{\omega - E_m + E_0 + i\delta} - \frac{\langle\Psi_n|\hat{\rho}(r_2)|\Psi_m\rangle\langle\Psi_m|\hat{\rho}(r_1)|\Psi_n\rangle}{\omega + E_m - E_0 - i\delta}\right], \end{aligned} \tag{3.28}$$

with the derivation for each R_n being identical to the non-degenerate one and where the summation over m is over all states except the degenerate ground state specified by n. As degenerate ground states are considered, m in Eq. (3.28) can specify a degenerate ground state separate from the one specified by n, and thus a divergence can be obtained for $\omega \to 0$. As such a divergence is not physical, we propose a diagonalization procedure.

The linear ensemble density response in Eq. (3.28) can be rewritten in the form:

$$R(r_1, r_2; \omega) = \sum_{\alpha,\beta} b_\alpha(r_1) R_{\alpha,\beta}(\omega) b_\beta(r_2), \tag{3.29}$$

$$R_{\alpha,\beta}(\omega) = \frac{1}{M} \sum_{n=1}^{M} \sum_{m \neq n} \left[\frac{\rho^\alpha_{nm} \rho^\beta_{mn}}{\omega - E_m + E_0 + i\delta} - \frac{\rho^\alpha_{mn} \rho^\beta_{nm}}{\omega + E_m - E_0 - i\delta} \right], \tag{3.30}$$

with a basis $b_\alpha(1) = \phi_i(1)\phi^*_j(1)$ and density matrix elements $\rho^\alpha_{nm} = \langle \Psi_n | c_i c^\dagger_j | \Psi_m \rangle$, and where α, β are collective indices specifying (i, j). By diagonalizing ρ^α, with $\rho^\alpha_{nn} = 0$ for all n as the sum is over $m \neq n$, in the degenerate subspace for each α one can construct new basis sets $|\Psi^\alpha\rangle$ which are eigenstates of ρ^α. Using the new constructed basis sets the terms which diverge for $\omega \to 0$ vanish. The diagonalization procedure is not in practice necessary to be utilized as the remaining terms are independent on the choice of degenerate ground state basis, leading to the following result:

$$R(r_1, r_2; \omega) = \frac{1}{M} \sum_{n=1}^{M} \sum_{m}^{\text{exci}} \left[\frac{\langle \Psi_n | \hat{\rho}(r_1) | \Psi_m \rangle \langle \Psi_m | \hat{\rho}(r_2) | \Psi_n \rangle}{\omega - E_m + E_0 + i\delta} - \frac{\langle \Psi_n | \hat{\rho}(r_2) | \Psi_m \rangle \langle \Psi_m | \hat{\rho}(r_1) | \Psi_n \rangle}{\omega + E_m - E_0 - i\delta} \right]. \tag{3.31}$$

In the case where the weights are not uniform, the diagonalization procedure can still be utilized. In this case, the remaining terms are, however, not in general independent of the choice of degenerate ground state basis as the weight becomes state-dependent and the sum over n no longer leads to a simple basis-independent trace over the degenerate ground states.

The choice of denominator in Eq. (3.2) is motivated by that this specific choice leads to the resulting sum in Eq. (3.28) being for $m \neq n$, in turn allowing for the proposed diagonalization procedure. This subtle point will be further discussed in section 3.1.4. The diagonalization procedure cannot be employed for each separate R_n, indicating their auxiliary nature. The linear ensemble density response functions is thus the only quantity of physical relevance, motivating the choice of Hartree potential as the ensemble one.

The fourth ensemble Hedin equation relates the ensemble polarization P to the Green's functions G_n and vertex functions Λ_n. The equation can be obtained from Eq. (3.24) by using the chain-rule for functional derivatives and partial integration, leading to

$$P(1,2) = -i \sum_n w_n \int d3d4 \; G_n(1,3) \Lambda_n(3,4,2) G_n(4,1^+) \; . \tag{3.32}$$

The final ensemble Hedin equation is obtained by rewriting Eq. (3.22) as,

$$\Lambda_n(1,2,3) = \delta(1-2)\delta(1-3) + \frac{\delta \Sigma_n(1,2)}{\delta V(3)}, \tag{3.33}$$

using the chain-rule for functional derivatives and partial integration. As in the non-degenerate case, the ensemble Hedin equations are an exact set of equations but not feasible to use for numerical computations, and approximations are thus required.

3.1.3 Ensemble *GW* approximation

To develop a computational scheme useful for electronic structure computations, we now propose an ensemble analogue of the GWA. We define the ensemble GWA as setting $\delta\Sigma_n/\delta V = 0$ in Eq. (3.33), corresponding to setting the vertex functions as

$$\Lambda_n(1,2,3) = \delta(1-2)\delta(1-3). \tag{3.34}$$

Two of the Hedin equations are modified (Eqs. (3.23) and (3.32)) under the ensemble GWA assumption:

$$\Sigma_n(1,2) = iG_n(1,2)W(2,1) + \delta(1-2)\left(V_n^H(1) - V^H(1)\right), \tag{3.35}$$

$$P(1,2) = -i\sum_n w_n G_n(1,2)G_n(2,1^+). \tag{3.36}$$

We further assume the RPA, leading to the ensemble analogue of the RPA equation,

$$R(1,2) = P^0(1,2) + \int d3\,d4\; P^0(1,3)v(3-4)R(4,2), \tag{3.37}$$

which in turn modifies Eq. (3.27):

$$W(1,2) = v(1-2) + \int d3\,d4\; v(1-3)P^0(3,4)W(4,2). \tag{3.38}$$

The non-interacting ensemble polarization is of the same form as the linear ensemble density response function, given by Eq. (3.31), with the non-interacting states and energies used instead of the interacting ones.

We will construct two computational schemes based on the ensemble GWA: A one-shot ensemble G^0W^0 approach and a self-consistent ensemble GW approach, outlined in Fig. 3.1, with a structure nearly identical to their non-ensemble counterparts, Fig. 2.2. The initial step in the ensemble G^0W^0 approach is the construction of the non-interacting states and energies from a self-consistent ensemble mean-field Hamiltonian. Thereafter, as in the non-degenerate case, the spin-polarized non-interacting Green's functions G_n^0 and the non-interacting ensemble polarization P^0 are computed, and in turn the ensemble screened interaction W. The spin-polarized self-energy Σ_n computation can be separated into an exchange and correlation part. The exchange part is given by:

$$\Sigma_n^x(1,2) = -v(1-2)\sum_m^{\mathrm{occ(n)}} \phi_m(1)\phi_m^*(2) + \delta(1-2)\left(V_n^H(1) - V^H(1)\right), \tag{3.39}$$

where the Green's functions have been set to the non-interacting ones and where occ(n) specifies the occupied orbitals of the non-interacting ground state $|\Psi_n\rangle$. The imaginary part of the correlation self-energy is given by

$$\mathrm{Im}\Sigma_n^c(r_1,r_2;\omega \le \mu) = -\sum_m^{\mathrm{occ(n)}} \phi_m(r_1)\phi_m^*(r_2)\mathrm{Im}W^c(r_1,r_2;\epsilon_m-\omega)\theta(\epsilon_m-\omega), \tag{3.40}$$

$$\mathrm{Im}\Sigma_n^c(r_1,r_2;\omega > \mu) = \sum_m^{\mathrm{unocc(n)}} \phi_m(r_1)\phi_m^*(r_2)\mathrm{Im}W^c(r_1,r_2;\omega-\epsilon_m)\theta(\omega-\epsilon_m), \tag{3.41}$$

using the non-interacting Green's functions and $W^c \equiv W - v$, and where unocc(n) specifies the unoccupied orbitals of the non-interacting ground state $|\Psi_n\rangle$. Defining the spectral functions Γ_n of the correlation self-energies as

$$\Gamma_n(r_1, r_2; \omega) = -\frac{1}{\pi}\text{sgn}(\omega - \mu)\text{Im}\Sigma_n^c(r_1, r_2; \omega), \tag{3.42}$$

as in the non-degenerate case, one can compute the real part of Σ_n as the Hilbert transform of Γ_n:

$$\text{Re}\Sigma_n^c(r_1, r_2; \omega) = P\int_{-\infty}^{\infty} d\omega' \frac{\Gamma_n(r_1, r_2; \omega')}{\omega - \omega'}. \tag{3.43}$$

The Green's function G can finally be computed from the G_n Green's functions, which are computed with the Dyson equations Eq. (3.21).

The self-consistent ensemble GW approach is an iterative approach built upon the ensemble G^0W^0 approach just as in the non-degenerate case. A difference relative to the non-degenerate case is the computation of the polarization P from the Green's functions G_n. In this step the diagonalization procedure is again required, which is equivalent to discarding the terms which diverge at $\omega \to 0$ as in the non-interacting computation. In each iteration there is a possible degeneracy breaking, which becomes a conceptual issue in a self-consistent scheme. To solve this, we propose to employ the Galitskii-Migdal formula on the auxiliary Green's functions and keeping the auxiliary Green's functions which gives the lowest ground state energy for iteration that follows. A possibility is also to introduce a minor mixing between the auxiliary Green's functions and the ensemble Green's function for the computation of the following iteration.

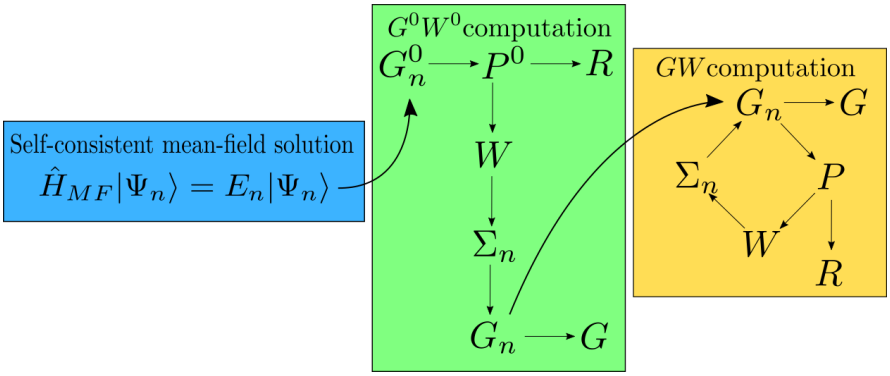

Figure 3.1: Diagrammatic view of the computational scheme used in the ensemble G^0W^0 and GW approach. The initial step (left) correspond to a self-consistent mean-field approach. The first iteration corresponds to the ensemble G^0W^0 approach (middle) and the iterative self-consistent approach corresponds to the ensemble GW approach (right).

For perturbation schemes other then the GW one, we anticipate additional complexicities appearing analogoues to the ones which appear in the standard Green's function theory. However, there are possibilities of introducing even further complexity as one works with a set of auxiliary Green's function G_n instead of a single one as in the standard case.

3.1.4 Ensemble linear response function

An essential ingredient in studying the physical properties of a many-electron system is the retarded linear response function, described in section 2.4 for the zero-temperature

case with a non-degenerate ground state. A *retarded* linear ensemble density response function, describing the change of the ensemble average expectation value of the density operator with respect to an external field, can be introduced. As in the non-degenerate case, the Kubo formula can be used to identify the form of the retarded linear ensemble density response function. Two equivalent forms of the retarded linear ensemble density response function in the Heisenberg picture are of interest in the upcoming discussion:

$$iR^r(1,2) = \frac{1}{M}\sum_{n=1}^{M}\langle\Psi_n|[\Delta\hat{\rho}(1),\Delta\hat{\rho}(2)]|\Psi_n\rangle\theta(t_1-t_2), \tag{3.44}$$

$$iR^r(1,2) = \frac{1}{M}\sum_{n=1}^{M}\langle\Psi_n|[\Delta\hat{\rho}_n(1),\Delta\hat{\rho}_n(2)]|\Psi_n\rangle\theta(t_1-t_2), \tag{3.45}$$

where $\Delta\hat{\rho}$ and $\Delta\hat{\rho}_n$ are defined as:

$$\Delta\hat{\rho}(1) = \hat{\rho}(1) - \rho(1), \quad \Delta\hat{\rho}_n(1) = \hat{\rho}(1) - \rho_n(1). \tag{3.46}$$

The form (3.44) is the standard form in literature, with structure similar to the one in the temperature formalism. Peaks at $\omega = 0$ from the excitations within the degenerate groundstate subspace do not appear in general in the retarded response function. A time-ordered version of Eq. (3.44) does not satisfy relations (2.28) and (2.29), as the diagonalization procedure cannot be employed. Instead, the proposed time-ordered linear ensemble density response function, given by Eq. (3.28), is the time-ordered version of Eq. (3.45). By the diagonalization procedure, the linear ensemble density response function (3.31) satisfies relations (2.28) and (2.29).

A subtle point is that the choice of denominator of the G_n in Eq. (3.2) leads to the diagonalization procedure to be applicable to linear ensemble density response function. For example, consider another choice of the denominator:

$$iG_n(1,2) = \frac{\langle\Psi_n|T[\hat{S}\hat{\psi}_D(1)\hat{\psi}_D^\dagger(2)]|\Psi_n\rangle}{\frac{1}{M}\sum_{n=1}^{M}\langle\Psi_n|\hat{S}|\Psi_n\rangle}. \tag{3.47}$$

The structure of the linear ensemble density response function is then modified by this alternative definition:

$$\begin{aligned} R(r_1,r_2;\omega) = \frac{1}{M}\sum_{n=1}^{M}\sum_{m}\Bigg[&\frac{\langle\Psi_n|\Delta\hat{\rho}(r_1)|\Psi_m\rangle\langle\Psi_m|\Delta\hat{\rho}(r_2)|\Psi_n\rangle}{\omega - E_m + E_0 + i\delta} \\ &- \frac{\langle\Psi_n|\Delta\hat{\rho}(r_2)|\Psi_m\rangle\langle\Psi_m|\Delta\hat{\rho}(r_1)|\Psi_n\rangle}{\omega + E_m - E_0 - i\delta}\Bigg]. \end{aligned} \tag{3.48}$$

Here the diagonalization procedure is not employable, therefore leading to the function in general not satisfying the relations required of a time-ordered response function. The natural connection of the linear ensemble density response function to the retarded one, is one of the main arguments for the choice of structure in the proposed formalism.

3.1.5 Ensemble spectral function

The treatment of the ensemble spectral function requires special care in the degenerate case. As reviewed in section 2.5, in the non-degenerate case the spectral function and

Green's function are related by Eqs. (2.40) and (2.41). In general, both equations are not necessarily satisfied. For example, in the non-interacting case the highest occupied and lowest occupied peak are positioned at the chemical potential μ. The imaginary parts of the occupied and unoccupied peaks will thus lead to cancellation in the imaginary part of the ensemble Green's function at μ. As an illustration of this fact, consider the non-interacting Green's functions G_n^0, given by:

$$G_n^0(r_1, r_2; \omega) = \sum_m^{\mathrm{occ}(n)} \frac{\phi_m^*(r_1)\phi_m(r_2)}{\omega - \epsilon_n - i\delta} + \sum_m^{\mathrm{unocc}(n)} \frac{\phi_m^*(r_1)\phi_m(r_2)}{\omega - \epsilon_n + i\delta}. \tag{3.49}$$

The difference between the ground states corresponds to electrons occupying different orbitals at the chemical potential μ. Therefore, in the non-interacting ensemble Green's function G^0, terms of the form

$$\frac{\phi_m^*(r_1)\phi_m(r_2)}{\omega - \mu - i\delta} + \frac{\phi_m^*(r_1)\phi_m(r_2)}{\omega - \mu + i\delta} = \phi_m^*(r_1)\phi_m(r_2)\frac{2(\omega - \mu)}{(\omega - \mu)^2 + \delta^2}, \tag{3.50}$$

will arise, with cancellation of the imaginary part. Furthermore in the general case, the sum rule (Eq. (2.43)) is not necessarily satisfied by the function defined by Eq. (2.40), as the peak structure at μ is partially to fully absent, implying the function is not the spectral function, defined by (2.37).

The main problem is that the occupied and unoccupied peaks are not introduced with the correct sign. We propose an approach to introduce the occupied and unoccupied peaks with the correct sign in the ensemble spectral function. Poles in the upper and lower imaginary plane are naturally separated in the spin-polarized G_n, thus we propose to instead compute the separate auxiliary spectral functions A_n from the Green's functions G_n. The sought ensemble spectral function A can then be computed as a weighted sum over the A_n functions.

3.2 Finite-temperature: Relationship and extension

A major problem in the construction of a general zero-temperature Green's function formalism which incorporates degenerate ground states is that the adiabatic connection is no longer obvious. This problem does not appear in the development of the temperature Green's function formalism. The adiabatic connection becomes irrelevant when working in imaginary time by employing the Matsubara Green's function, see section 2.6. In the limit of $T \to 0^+$, the exploited periodicity is lost and no benefits are obtained by working in the regime of imaginary time in the zero-temperature case. Treatment of the temperature case was previously limited to systems of non-degenerate states. However, the degeneracy of the ground state (and excited states) is naturally incorporated in the grand canonical ensemble of the temperature formalism. The purpose of this section is to relate the ensemble formalism with the finite-temperature formalism in the limit of $T \to 0^+$, and to propose an extension of the finite-temperature Green's function theory to systems with degenerate states.

The natural comparison of the ensemble and finite-temperature Green's function theory is the real-time analogues. The Matsubara Green's function in imaginary-time does not have an analogous function in the ensemble formalism. Taking $T \to 0^+$ for the

real-time Green's function, given by Eq. (2.92), one obtains:

$$\bar{G}(1,2) = -i\frac{1}{M}\sum_{n=1}^{M}\langle\Psi_n|T[\hat{\psi}_K(1)\hat{\psi}_K^\dagger(2)]|\Psi_n\rangle \equiv \frac{1}{M}\sum_{n=1}^{M}\bar{G}_n(1,2). \tag{3.51}$$

This equation is of the same form as the definition of the ensemble Green's function, Eqs. (3.1) and (3.2), in the Heisenberg picture with equal weights $w_i = 1/M$, except with the modified Hamiltonian $\hat{K}$ used instead.

The retarded linear response function constructed by the Kubo formula (Eq. (2.93)) does not contain divergences at $\omega = 0$ for finite temperature. However, for many-electron systems with degenerate states the linear density response function of the form (2.95) in general diverges as $\omega \to 0$. As a diagonalization procedure cannot be employed, the function (2.95) does not satisfy the relations (2.28) and (2.29). An equivalent rewritten form of the retarded linear density response function is the following in the modified Heisenberg picture:

$$iR^r(1,2) = \mathrm{Tr}\left\{\hat{\rho}_G[\Delta\hat{\rho}_n(rt), \Delta\hat{\rho}_n(r't')]\right\}\theta(t-t'), \tag{3.52}$$

where $\Delta\hat{\rho}_n$ is defined as:

$$\Delta\hat{\rho}_n(1) = \hat{\rho}(1) - \langle\Psi_n|\hat{\rho}(1)|\Psi_n\rangle. \tag{3.53}$$

A time-ordered linear density response function based on Eq. (3.52) can in the spectral representation be written as:

$$\begin{aligned} R(r,r';\omega) = Z_G^{-1}\sum_{n\neq m}&\langle\Psi_n|\rho(r)|\Psi_m\rangle\langle\Psi_m|\rho(r')|\Psi_n\rangle \\ &\times\left[\frac{e^{-\beta K_n}}{\omega - K_m + K_n + i\delta} - \frac{e^{-\beta K_m}}{\omega - K_m + K_n - i\delta}\right], \end{aligned} \tag{3.54}$$

derived in the same fashion as for the time-ordered linear density response function for systems of non-degenerate states treated in section 2.5. The function (3.54) is a more natural definition of the linear density response function, as the diagonalization procedure can be employed, and thus the relations (2.28) and (2.29) are satisfied, implying its validity. In the limit of $T \to 0^+$ the linear density response (3.54), with the diagonalization procedure employed, acquires an identical form to the ensemble linear density response function (3.31), with $\hat{K}$ used instead of $\hat{H}$.

A modification of the standard form of the interaction picture Matsubara Green's function (Eq. (2.91)) is required for a natural connection to the linear density response function of the form (3.54), which would not be obtained in the standard form. We propose the following modified form of the Matsubara Green's function in the interaction picture:

$$\mathcal{G}(1,2) = \sum_n w_n\mathcal{G}_n(1,2), \quad w_n = \frac{e^{-\beta K_n}}{Z_G} \tag{3.55}$$

with $\mathcal{G}_n$ Matsubara Green's functions defined as

$$\mathcal{G}_n(1,2) = -\frac{\langle\Psi_n|e^{-\beta\hat{K}_0}T_\tau\left[\hat{\mathcal{U}}(\beta,0)\hat{\psi}_I(1)\hat{\psi}_I^\dagger(2)\right]|\Psi_n\rangle}{\langle\Psi_n|e^{-\beta\hat{K}_0}\hat{\mathcal{U}}(\beta,0)|\Psi_n\rangle}, \tag{3.56}$$

compare with standard form (2.91) where one traces separately over the numerator and denominator. A computational approach similar to the ensemble one for zero-temperature can be constructed in the finite-temperature regime for a general electronic system with degenerate states. An extended finite-temperature formalism which contains the ensemble formalism has thus been proposed.

Chapter 4

Results

The current chapter details the application of the ensemble G^0W^0 computational scheme on four model systems: a three-orbital Hubbard model, a two-dimensional harmonic oscillator system, an Ising model system and a hydrogen-like system. The chapter begins with a description of the implementation of the computational scheme. The remaining sections of the chapter focus on the application to the four model systems.

4.1 Implementation

The implementation of the ensemble G^0W^0 computational scheme can be divided into two parts. The first part involves a construction of the one-particle orbitals and the states, with a computation of corresponding energies obtained using a mean-field ensemble Hamiltonian approach. The second part involves the implementation of the ensemble G^0W^0 computational scheme, with the many-electron energies and states of the first part as input. In the current section, the description of the implementation will be divided similarly, and a description of the exact computation will be included as well. A modified approach will be discussed in a later section for the Ising model.

In the exact case, the sought states and their corresponding energies correspond to the eigenvectors and eigenvalues of the Hamiltonian matrix H, defined by,

$$H_{nm} = \langle \Psi_n | \hat{H} | \Psi_m \rangle. \tag{4.1}$$

To construct the Hamiltonian matrix, the interaction four-index matrix v_{ijkl}, defined by,

$$v_{ijkl} \equiv \int d1\, d2\; \phi_i^*(1)\phi_j^*(2)v(1-2)\phi_k(2)\phi_l(1), \tag{4.2}$$

needs to be constructed. In the current thesis the interaction v_{ijkl} is constructed either from known orbitals of a model system with a defined interaction v, or by a comparison between the Hamiltonian of a model system with an implicit dependence on the orbital and the many-electron Hamiltonian (Eq. (2.2)). The diagonalization of the Hamiltonian is required to be done for N, $N+1$ and $N-1$ electrons, to describe photoemission and inverse photoemission, in order to compute the Green's function.

In the non-interacting case, the energies are computed by a mean-field ensemble Hamiltonian approach. Initial many-electron energies are computed as the sum of the one-electron energies, and used to compute the ensemble Hartree potential with the interaction v_{ijkl}. The many-electron energies are then modified by the potential, and a new

ensemble density can be computed for a new set of ground states. In the self-consistent mean-field approach used in the thesis, the employed ensemble Hartree potential is a mixture of the old and new ensemble Hartree potential. This iterative approach is then continued until the degenerate ground states or non-degenerate ground state, satisfying the symmetry of the ensemble Hartree potential, is obtained. In the non-interacting case, it is enough to construct the states with corresponding many-electron energies of the N electron system.

In the current thesis, the main quantities of interest are the ensemble Green's function and linear ensemble density response functions. For a basis $\{\phi_i(r)\}$, Hedin's equations can be expressed as a set of matrix equations. Assuming repeated indices are summed over, except n which labels degeneracy, the matrix form of the Hedin's equations, within GWA and RPA, can be written as:

$$G_{n,ij}(\omega) = G^0_{n,ij}(\omega) + G^0_{n,ik}(\omega)\Sigma_{n,kl}(\omega)G_{n,lj}(\omega), \tag{4.3}$$

$$\Sigma^x_{n,ij}(\omega) = -\sum_m^{\text{occ(n)}} v_{imjm} + \sum_m^{\text{occ(n)}} v_{immj} - \frac{1}{M}\sum_{m=1}^{M}\sum_k^{\text{occ(m)}} v_{ikkj}, \tag{4.4}$$

$$\text{Im}\Sigma^c_{n,ij}(\omega \leq \mu) = -\sum_m^{\text{occ(n)}} \text{Im}W^c_{imjm}(\epsilon_m - \omega)\theta(\epsilon_m - \omega), \tag{4.5}$$

$$\text{Im}\Sigma^c_{n,ij}(\omega > \mu) = \sum_m^{\text{unocc(n)}} \text{Im}W^c_{imjm}(\omega - \epsilon_m)\theta(\omega - \epsilon_m), \tag{4.6}$$

$$W_{\alpha\beta}(\omega) = v_{\alpha\beta} + v_{\alpha\gamma}P^0_{\gamma\delta}(\omega)W_{\delta\beta}(\omega), \tag{4.7}$$

$$R_{\alpha\beta}(\omega) = P^0_{\alpha\beta} + P^0_{\alpha\gamma}(\omega)v_{\gamma\delta}R_{\delta\beta}(\omega), \tag{4.8}$$

where α is the collective index (i, j) etc. and the matrices are defined by:

$$G_n(r_1, r_2; \omega) \equiv \phi^*_i(r_1)G_{n,ij}(\omega)\phi_j(r_2), \tag{4.9}$$

$$\Sigma_{n,ij}(\omega) \equiv \int d1\, d2\ \phi^*_i(r_1)\Sigma_n(r_1, r_2; \omega)\phi_j(r_2), \tag{4.10}$$

$$W_{ijkl}(\omega) \equiv \int d1\, d2\ \phi^*_i(r_1)\phi^*_j(r_2)W(r_1, r_2; \omega)\phi_k(r_2)\phi_l(r_1), \tag{4.11}$$

$$R(r_1, r_2; \omega) \equiv \phi^*_i(r_1)\phi_j(r_1)R_{ijkl}(\omega)\phi^*_k(r_2)\phi_l(r_2). \tag{4.12}$$

The form of the definition of W^c_{ijkl} and P^0_{ijkl} is identical to that of W_{ijkl} and R_{ijkl}, respectively. In the exact case the interacting states and energies are used to compute the G and R matrices using Eqs. (3.5) and (3.31). In the G^0W^0 approach, the spin-polarized G^0_n and P^0 are computed using Eqs. (3.5) and (3.31), with the scheme then following the approach described in section 3.1 to compute the matrices G and R.

To compare the result of different approaches, the ensemble spectral function A (Eq. (2.37)) and the spectral form S (Eq. (2.66)) of the linear ensemble density response function R are computed. The matrix forms are computed for A and S, defined by:

$$A(r_1, r_2; \omega) \equiv \phi^*_i(r_1)A_{ij}(\omega)\phi_j(r_2), \tag{4.13}$$

$$S(r_1, r_2; \omega) \equiv \phi^*_i(r_1)\phi_j(r_1)S_{ijkl}(\omega)\phi^*_k(r_2)\phi_l(r_2). \tag{4.14}$$

The elements A_{ij} and S_{ijkl} are basis-dependent. To make a comparison between different approaches the basis-independent trace of A and S are computed:

$$\mathrm{Tr}A(\omega) = \sum_i A_{ii}(\omega), \quad \mathrm{Tr}S(\omega) = \sum_{ij} S_{ijji}(\omega). \tag{4.15}$$

4.2 Hubbard model

We consider the Hubbard model, first introduced by Hubbard in [34], with three-orbitals. The three-orbital model is an analytically solvable model in both the exact and G^0W^0 approach. The mechanics of the Hubbard model is defined by the Hamiltonian of the form:

$$\hat{H} = \sum_{ij\sigma} t_{ij}\hat{c}^\dagger_{i\sigma}\hat{c}_{j\sigma} + \sum_i U_i \hat{n}_{i\uparrow}\hat{n}_{i\downarrow}, \tag{4.16}$$

with an implicit orbital dependence from the hopping parameter t_{ij} and on-site interaction U_i, and where $\hat{n}_{i\sigma} = \hat{c}^\dagger_{i\sigma}\hat{c}_{i\sigma}$ is the particle number operator for orbital i with spin σ. The Hubbard model is a common model for describing conducting and insulating systems together with the transition between the two regimes. We specialize to three orbitals with a Hamiltonian of the form:

$$\hat{H} = \sum_{i\sigma} \epsilon_i \hat{c}^\dagger_{i\sigma}\hat{c}_{i\sigma} + U\sum_i \hat{n}_{i\uparrow}\hat{n}_{i\downarrow}, \tag{4.17}$$

with the one-electron energies ϵ_i for the three orbitals and with an identical on-site interaction U for all orbitals. The system is composed of two lower orbitals ϕ_1, ϕ_2 with an energy $\epsilon_1 = \epsilon_2 = 0$ and one third orbital ϕ_3 with a positive energy $\epsilon_3 = \epsilon$.

A two-electron system is considered. The interacting ground states has a double degeneracy for both an attractive and repulsive on-site interaction, corresponding to $U < 0$ and $U > 0$, respectively. In the special case of $U = 0$, corresponding to a non-interacting ground state, the degeneracy is four-fold. The possible interacting ground states correspond to both electrons occupying the two lower orbitals, see Fig. 4.1. For $U < 0$ the double degeneracy consist of the double occupied orbitals, while for $U > 0$ the double degeneracy consist of the states with electrons occupying different orbitals. The non-interacting ground states have a four-fold degeneracy spanned by all states with two electrons occupying the two lowest orbitals, for $U < \epsilon$ and independent of the sign of U, with the self-consistent ensemble Hartree mean-field approach not converging for $\epsilon \leq U$. We will specialize to case of the repulsive on-site interaction in the current section.

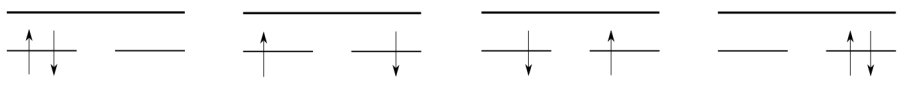

Figure 4.1: The possible ground states in the repulsive and attractive U regime in the considered three-orbital Hubbard model.

In the exact case, the non-vanishing elements of the ensemble linear-density response function R can be constructed from the $N = 2$ electron states as

$$R_{12,12}(\omega) = \frac{2}{\omega - U + i\delta} - \frac{2}{\omega + U - i\delta}, \tag{4.18}$$

$$R_{13,13}(\omega) = R_{23,23}(\omega) = \frac{1}{\omega - \epsilon + i\delta} - \frac{1}{\omega + \epsilon - i\delta}. \tag{4.19}$$

Here the orbitals can be assumed to be real-valued, allowing for reordering of the indicies to construct a diagonal matrix R. The ensemble Green's function is computed from the $N = 2$ electron states as well as the $N - 1$ and $N + 1$ electron states, obtaining the exact form:

$$G_{11}(\omega) = G_{22}(\omega) = \frac{1}{\omega - i\delta} + \frac{1}{\omega - U + i\delta}, \tag{4.20}$$

$$G_{33}(\omega) = \frac{2}{\omega - \epsilon + i\delta}. \tag{4.21}$$

The electron affinity μ is observed to be located between 0 and U, for $0 < U < \epsilon$, and between 0 and ϵ, for $\epsilon < U$, by using the sum-rules for the spectral function.

The ensemble G^0W^0 computation is now considered for $U < \epsilon$. The non-vanishing elements of the non-interacting ensemble polarization P^0 can be constructed as:

$$P^0_{13,13}(\omega) = P^0_{23,23}(\omega) = \frac{1}{\omega - (\epsilon - U) + i\delta} - \frac{1}{\omega + (\epsilon - U) - i\delta}. \tag{4.22}$$

The R and W are obtained as identical to P^0 and v, respectively, in the current case, and thus only the exchange part of the self-energy is non-zero. The G is obtained in the G^0W^0 scheme as:

$$G^{GW}_{11}(\omega) = G^{GW}_{22}(\omega) = \frac{1}{2}\left(\frac{1}{\omega - U - i\delta} + \frac{1}{\omega - i\delta}\right) + \frac{1}{\omega + i\delta}, \tag{4.23}$$

$$G^{GW}_{33}(\omega) = \frac{2}{\omega - \epsilon + i\delta}. \tag{4.24}$$

The electron affinity is observed to be located at $\mu = 0$.

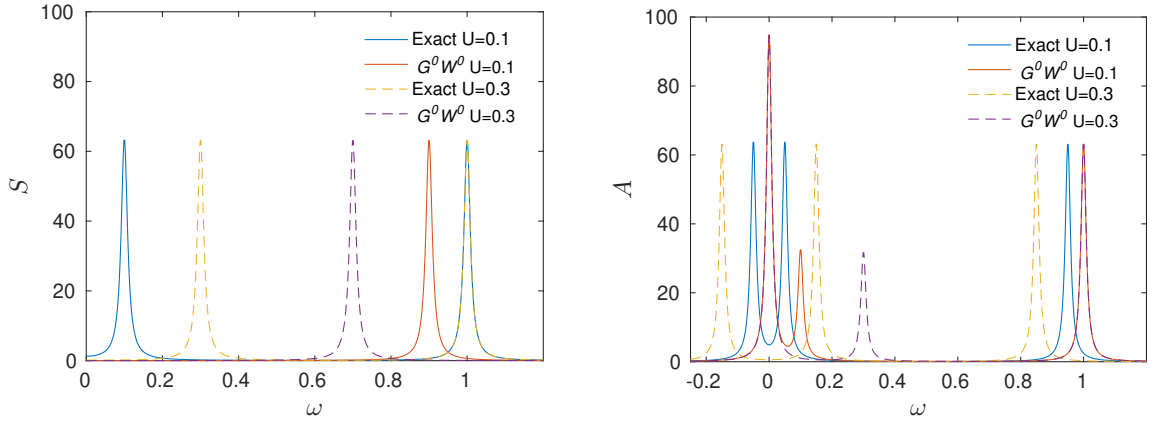

Figure 4.2: The TrS (left) and TrA (right) plotted against the energy ω for the exact approach and the ensemble G^0W^0 approach, with on-site interactions $U = 0.1$ and $U = 0.3$, and with $\delta = 0.01$. The spectral response function is anti-symmetric around $\omega = 0$ and the electron affinity of the spectral functions are shifted to $\mu = 0$.

The functions TrS and TrA are plotted in the considered cases in Fig. 4.2 for $\epsilon = 1$ and with $U = 0.1$ and $U = 0.3$. The electron affinity is specified as $\mu = U/2$ for the exact case, to illustrate the difference between the exact and ensemble G^0W^0 results. While the peak in TrS from transitions between the lower orbitals to the higher orbital is captured in the G^0W^0 scheme, the peak from transitions between the two lowest orbitals in the

degenerate subspace is neglected by the diagonalization procedure. The captured peak of TrS is shifted towards lower energies in the ensemble G^0W^0 scheme relative the exact peak, with the shift increasing and agreement worsening as U increases towards ϵ relative the exact peak, which has a peak position independent of U. There is partial agreement in the main peak structure in TrA computed in the two approaches, with two peaks around the electron affinity and a single higher energy peak. However, a clear problem with the ensemble G^0W^0 approach is the predicted electron affinity in the middle of a peak, thus predicting a metallic system, which is not observed in the exact result.

The main results for the simple three-orbital Hubbard model is the illustration of the application of the ensemble formalism. Peaks in the exact case originating from transitions between states which are part of the degenerate subspace in the non-interacting mean-field ensemble Hamiltonian are removed by the diagonalization procedure. Peaks originating from the breaking of the symmetry going from non-interacting to interacting states can thus not be captured in the ensemble one-shot G^0W^0 scheme. The diagonalization scheme is not the source of the problem, as it corresponds to simply rotating the degenerate ground states in the degenerate subspace. We argue that the origin of the problem instead arises from the mean-field approach. The ensemble Hartree does not capture the repulsive/attractive nature of the interaction, leading to a four-fold degeneracy appearing in the non-interacting case. To capture the low ω peak structure in the response function, a mean-field approach which captures the repulsive/attractive nature would be required. We want to stress that the discussion of the failure of the ensemble formalism to capture the peak is specifically the ensemble one-shot G^0W^0 scheme. We expect that the peak structure originating from the symmetry breaking can be captured in a self-consistent approach, as the symmetry which may be broken in the computation of the self-energies Σ_n will be incorporated in the following iteration of the computation of the polarization.

4.3 Two-dimensional harmonic oscillator

We consider now a four-electron problem, with electrons moving in a two-dimensional harmonic potential. The one-electron energies of the two-dimensional harmonic oscillator are given by

$$\epsilon_{n_x,n_y} = \omega_0(n_x + n_y + 1), \tag{4.25}$$

with states specified by the quantum numbers $\{(n_x, n_y) = 0, 1, 2, ...\}$ and where ω_0 is the quantum energy of the harmonic oscillator, which we set to $\omega_0 = 1$. The orbital ϕ_{n_x,n_y} in the two-dimensional harmonic oscillator are known:

$$\phi_{n_x,n_y}(\mathbf{r}) = \phi_{n_x}(r_x)\phi_{n_y}(r_y), \tag{4.26}$$

$$\phi_n(t) = \frac{1}{\sqrt{2^n n!}} \left(\frac{1}{\pi}\right)^{1/4} e^{-\frac{t^2}{2}} H_n(t)\,, \tag{4.27}$$

with the *Hermite polynomials* H_n defined by:

$$H_n(t) = (-1)^n e^{t^2} \frac{d^n}{dt^n}\left(e^{-t^2}\right), \;\; n = 0, 1, 2, ... \;. \tag{4.28}$$

The electron-electron interaction is modeled as a point interaction of the form $v(\mathbf{r} - \mathbf{r}') = U\delta(\mathbf{r} - \mathbf{r}')$, where U is an interaction parameter.

Two different restricted sets of orbitals are treated, with the cases being the following:

- Three-orbital problem: Considering only the orbitals ϕ_{00}, ϕ_{01} and ϕ_{10} with energies $\epsilon_{00} = 1$, $\epsilon_{01} = 2$ and $\epsilon_{10} = 2$, respectively.
- Six-orbital problem: Considering only the orbitals ϕ_{00}, ϕ_{01}, ϕ_{10}, ϕ_{20}, ϕ_{11} and ϕ_{02} with energies $\epsilon_{00} = 1$, $\epsilon_{01} = \epsilon_{10} = 2$, $\epsilon_{20} = \epsilon_{11} = \epsilon_{02} = 3$, respectively.

The interaction elements v_{ijkl} are separated into separate integrations over r_x and r_y of polynomials multiplied by Gaussians, and are thus analytically solvable. As the orbitals are real-valued, the matrix form of R can be constructed in a diagonal form.

For both the three- and six-orbital case, the interacting ground state is non-degenerate and the non-interacting ground states has a four-fold degeneracy. The degenerate non-interacting ground state subspace is spanned by states with double occupation in the orbital ϕ_{00}, and two electrons occupying one or both orbitals ϕ_{01}, ϕ_{10}, see Fig. 4.3.

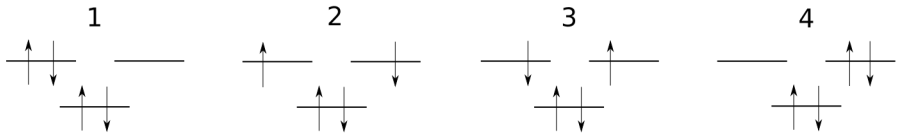

Figure 4.3: The four non-interacting degenerate ground states, numbered from 1 to 4, in the two-dimensional harmonic oscillator with only the orbitals corresponding to the two lowest non-interacting one-electron energies drawn.

Apart from the treatment of the ensemble G^0W^0 and the exact computations, a treatment of two alternative non-ensemble G^0W^0 computations will be considered. Choosing a state out of a set of degenerate states is by nature ill-defined as the degeneracy can be ignored in multiple different non-equivalent approaches. In approach A, one of the four non-interacting degenerate states is treated as a non-degenerate state, with the remaining ones ignored. The non-degenerate state is used to compute a new set of non-interacting energies. The choice of ground state is still somewhat ill-defined in the approach, as there is freedom in the ordering of the new basis. We specify the degenerate states by numbering them from 1 to 4, see Fig. 4.3. Beyond double occupation in orbital ϕ_{00}, state 1 and 4 have double occupation in orbital ϕ_{10} and ϕ_{01}, and state 2 has a spin-up and spin-down electron occupying ϕ_{10} and ϕ_{01}, respectively, and vice versa for state 3. In approach B, which is more well-defined, new sets of non-interacting ground states are computed for each of the four-degenerate states separately. We then chose the new set of non-interacting energies as the one giving a non-degenerate ground state with lowest energy. The standard G^0W^0 approach is then employed for both the A and B non-ensemble approaches.

We compute the traces TrS and TrA in the three-orbital case in the exact approach, and the ensemble and non-ensemble G^0W^0 approaches. The traces TrS and TrA are plotted as functions of energy for $U = 1.0$, shown in Figs. 4.4. An identical peak structure in TrS is observed for the ensemble approach and the non-ensemble A approach for states 2 and 3, with the spectrum constituting a single peak a bit below $\omega = 1$. The peak is in very good agreement with the exact approach. The non-ensemble A approaches for states 1 and 4 predict a single peak as well, however the peak positions are in worse agreement, while the non-ensemble B approach incorrectly predicts two peaks. For the trace TrA, the main peak structure of the exact approach, composed of two peaks at lower energy ω and a peak above and below the electron affinity, are captured by the ensemble approach and

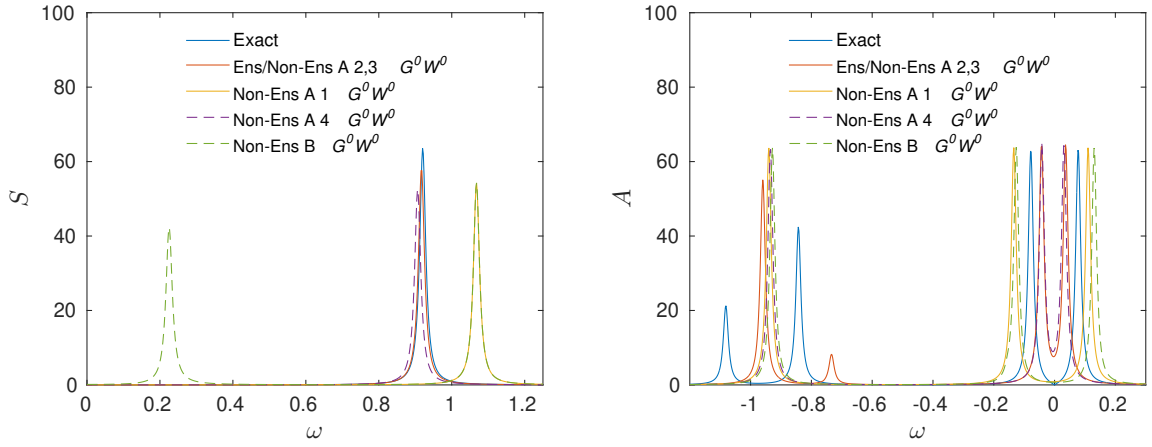

Figure 4.4: The TrS (left) and TrA (right) plotted against the energy ω in the three-orbital problem in the exact approach, and ensemble and non-ensemble G^0W^0 approaches, with $U = 1$ and $\delta = 0.01$. The finite size of delta function slightly shifts the electron affinity of the exact TrA, and this incorrect shift has been corrected for manually. The spectral response function is anti-symmetric around $\omega = 0$ and the electron affinity of the spectral functions are shifted to $\mu = 0$.

non-ensemble A approach for states 2 and 3. The peaks close to the electron affinity are captured, while the lower peaks are shifted towards $\omega = 0$. The remaining non-ensemble approaches capture a two peak structure close to the electron affinity, however they only predict one peak at lower energies.

The six-orbital problem was treated in the same way, with the traces TrS and TrA plotted as functions of energy for $U = 1.0$, shown in Figs. 4.5 and 4.5. While the peak structure of the two traces varies with respect to their three-orbital counterparts, the resulting discussion of the agreement between the different approach is similar. An identical peak structure in TrS is observed for the ensemble approach and the non-ensemble A approach for states 2 and 3, with this being in best agreement with the exact results. Some peak structures captures by the non-ensemble approaches are however not captures by the ensemble approach. A two peak structure at $\omega = 1.9$ is only captured by the non-ensemble A approach for states 1 and 4 and non-ensemble B approach, while the other approximate approaches only captures a single peak. The non-ensemble B approach incorrectly predicts a low energy peak. In the TrA spectrum, the agreement between the different G^0W^0 approaches varies over the energy range. The ensemble G^0W^0 is in reasonable agreement with the exact results. A two peak structure at the electron affinity and a three peak structure at $\omega = 1$ are captured well. Smaller satellites are not captures as well by the approach, however the ensemble approach is the only one predicting the single peak above $\omega = 2$. In contrast, a pair of peaks at $\omega = -1$ in the exact spectrum are better captured by the non-ensemble A approach for state 1 and non-ensemble B approach.

The main result in both the three- and six-orbital case is that the ensemble formalism captures features of the exact result in a well-defined approach. The non-ensemble formalism A gave in certain scenarios the same results as the ensemble one, however this formalism is in contrast ill-defined, as it depends on a choice of state. A property of interest in the two-dimensional harmonic oscillator is the transition from the degeneracy of the non-interacting ground states to a non-degenerate interacting ground state. The comparison in this section has thus also been a comparison between the ensemble and standard

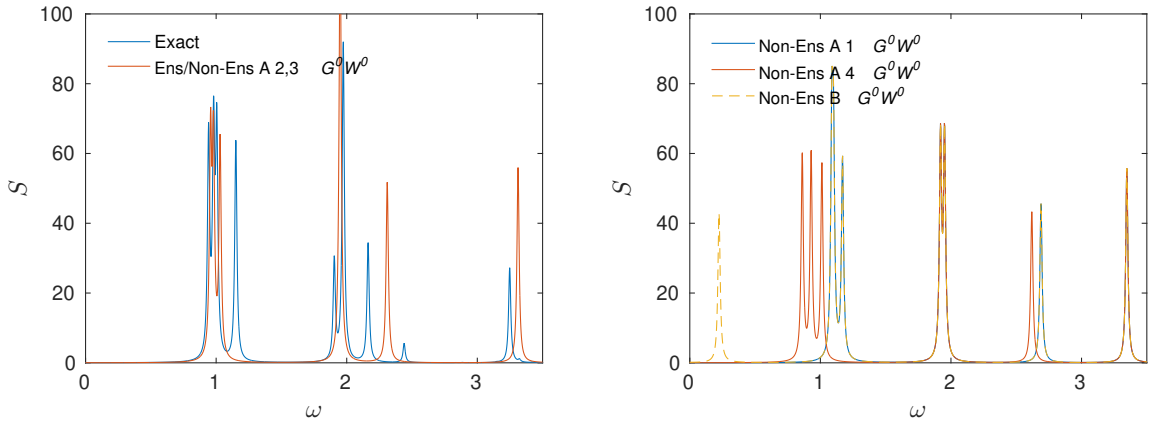

Figure 4.5: The TrS is plotted against the energy ω in the six-orbital problem in the exact approach, and ensemble and non-ensemble G^0W^0 approaches, with $U = 1$ and $\delta = 0.01$. The spectral response function is anti-symmetric around $\omega = 0$.

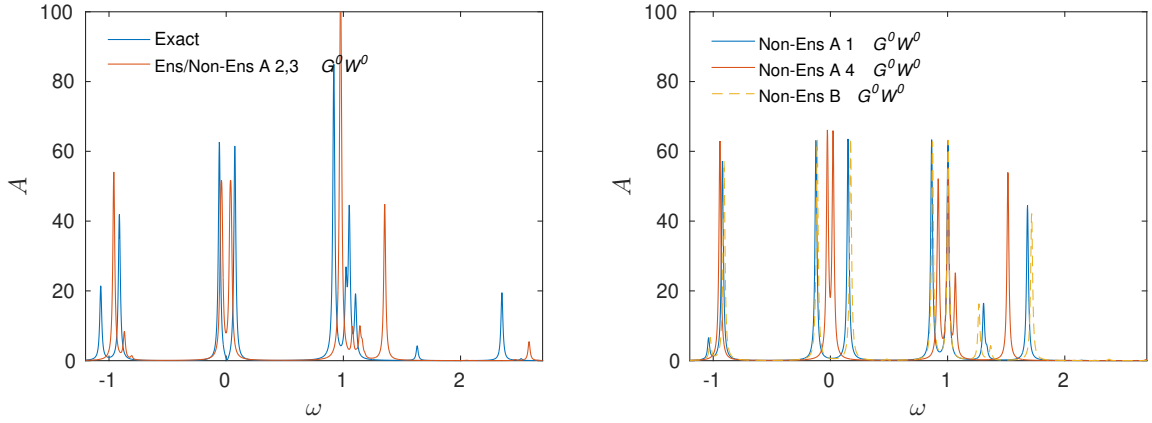

Figure 4.6: The TrA plotted against the energy ω in the six-orbital problem in the exact approach, and ensemble and non-ensemble G^0W^0 approaches, with $U = 1$ and $\delta = 0.01$. The finite size of delta function slightly shifts the electron affinity of the exact TrA. The electron affinity in this case has been shifted to correct for this error. The electron affinity of the spectral functions are shifted to $\mu = 0$.

Green's function theories. In contrast to the Hubbard model, a peak structure at low ω, originating from the breaking of the degeneracy in the transition from non-interacting states to interacting states, was not observed. Thus, the absence of a peak structure originating from the employment of the diagonalization procedure is not observed.

4.4 Ising model

An Ising model on a triangular lattice, first studied by Wannier in [35], will now be considered as an illustration of the application of the proposed formalism to a frustrated system. The Ising model is generally used for modeling of ferromagnetic and antiferromagnetic

systems. The mechanics of the Ising model is defined by the Hamiltonian:

$$\hat{H} = -\sum_{\langle i,j \rangle} J_{ij} \hat{S}_{zi} \hat{S}_{zj} - h \sum_{i} \hat{S}_{zi}, \tag{4.29}$$

with an implicit orbital-dependence from the interaction parameter J_{ij} and external magnetic field h along the z-direction, and where the sum over $\langle i,j \rangle$ specifies a sum over nearest neighbors, and where $\hat{S}_{zi}$ is the spin operator in the z-direction at site i. In constrast to previous systems, a site only allows for the occupation of a single electron. We will limit our considerations to a triangular lattice, with $J = J_{ij}$ for all i, j. The Ising model is described by a Hamiltonian with a spin-dependent two-electron interaction. The general form of the two-electron part of the Hamiltonian will be considered as:

$$\hat{H}_{2-electron} = \frac{1}{2} \sum_{\alpha\beta\gamma\delta} \int d^3r d^3r' \hat{\psi}^\dagger_\alpha(\mathbf{r}) \hat{\psi}^\dagger_\gamma(\mathbf{r}') v_{\alpha\beta\gamma\delta}(\mathbf{r}, \mathbf{r}') \hat{\psi}_\delta(\mathbf{r}') \hat{\psi}_\beta(\mathbf{r}), \tag{4.30}$$

where $\alpha, \beta, \gamma, \delta$ are spin-up or down. For more information regarding the Green's function method for spin-dependent interaction see for example [33].

Our goal is to compute the *linear charge and magnetic response* with respect to a perturbative external electromagnetic potential in both an exact approach and a RPA approach. The external perturbative potential is defined as:

$$\hat{\phi}(t) = \int d^3r \hat{\vec{\sigma}}(r,t) \cdot \vec{\varphi}(r,t), \tag{4.31}$$

with an electromagnetic four-field $\vec{\varphi} = (\varphi^0, \varphi^+, \varphi^-, \varphi^z)$ and with $\hat{\vec{\sigma}}$ defined as,

$$\hat{\vec{\sigma}}(r,t) = \sum_{\alpha\beta} \hat{\psi}^\dagger_\alpha(r,t) \vec{\sigma}_{\alpha\beta} \hat{\psi}_\beta(r,t), \tag{4.32}$$

where α, β are spin-up or down, and with four-vector $\vec{\sigma} = (\sigma^0, \sigma^+, \sigma^-, \sigma^z)$ composed of the Pauli spin matrices. The Pauli spin matrix convention used in the current thesis is the following one:

$$\sigma^0 = \begin{pmatrix} 1 & 0 \\ 0 & 1 \end{pmatrix}, \ \sigma^+ = \begin{pmatrix} 0 & 2 \\ 0 & 0 \end{pmatrix}, \ \sigma^- = \begin{pmatrix} 0 & 0 \\ 2 & 0 \end{pmatrix}, \ \sigma^z = \begin{pmatrix} 1 & 0 \\ 0 & -1 \end{pmatrix}. \tag{4.33}$$

The operator coupled to the electric field φ^0 is the density operator, leading to a term of the form (2.20). The operators coupled to the magnetic fields φ^+ and φ^- are connected to spin-flip operation, thus allowing connections to different states of the Ising model. The operator coupled to the magnetic field φ^z is the spin-density operator. It is convenient to write the interaction as an expansion in a basis of Pauli spin matrices:

$$v_{\alpha\beta\gamma\delta}(1,2) = \sum_{ij} \sigma^i_{\alpha\beta} v_{ij}(1,2) \sigma^j_{\gamma\delta}. \tag{4.34}$$

For the Ising model, the *charge* and *magnetic* response function and polarization will be under consideration using the proposed ensemble formalism. The linear ensemble charge and magnetic response function and ensemble polarization are defined as:

$$R_{ij}(1,2) \equiv \frac{\delta \langle \hat{\sigma}^i(1) \rangle}{\delta \varphi_j(2)}, \quad P_{ij}(1,2) \equiv \frac{\delta \langle \hat{\sigma}^i(1) \rangle}{\delta V_j(2)}, \tag{4.35}$$

where the expectation value is the ensemble one and where $V_i \equiv V_i^H + \varphi_i$, with V_i^H being a *generalized* Hartree potential, defined as:

$$V_i^H(1) = \sum_j \int d2 v_{ij}(1,2)\langle\hat{\sigma}^j(2)\rangle. \tag{4.36}$$

By a Schwinger functional derivative approach, the linear charge and magnetic response function can be written in the form:

$$R_{ij}(1,2;\omega) = \frac{1}{M}\sum_{n=1}^{M}\sum_{m}^{\text{exci}}\left[\frac{\langle\Psi_n|\hat{\sigma}^i(1)|\Psi_m\rangle\langle\Psi_m|\hat{\sigma}^j(2)|\Psi_n\rangle}{\omega - E_m + E_0 + i\delta} - \frac{\langle\Psi_n|\hat{\sigma}^j(2)|\Psi_m\rangle\langle\Psi_m|\hat{\sigma}^i(1)|\Psi_n\rangle}{\omega + E_m - E_0 - i\delta}\right], \tag{4.37}$$

see Appendix C for a derivation. By assumption of the RPA, a RPA equation between the response and non-interacting polarization can be constructed as,

$$R_{ij}(1,2) = P_{ij}^0(1,2) + \sum_{kl}\int d3d4 P_{ik}^0(1,3)v_{kl}(3,4)R_{lj}(4,2). \tag{4.38}$$

The non-interacting polarization is of the form (4.37), with non-interacting states and energies used instead. We will compute the non-interacting states and energies by applying *Mean-Field Theory* (MFT). The mean-field Hamiltonian of the Ising model is given by,

$$\hat{H}^{MF} = -J\sum_{\langle i,j\rangle}\left(2m\hat{S}_{zi} - m^2\right) - h\sum_i \hat{S}_{zi}, \tag{4.39}$$

with m being the mean-value of $m_i = \langle\hat{S}_{zi}\rangle$.

We now consider a three-site triangular lattice Ising model with all three sites having two neighbors. We specialize to $J < 0$, corresponding to antiparallel pairing between neighbouring spins being prefered. Choosing $-(2J/3) > h > 0$, both the interacting and non-interacting ground states are spanned by the states with total spin $\frac{1}{2}$, giving a three-fold degeneracy. In the exact case, the non-vanishing linear response functions are R_{-+} and R_{+-}, with the non-vanishing matrix elements:

$$R_{-+}^{xx,xx}(\omega) = -\left[R_{+-}^{xx,xx}(\omega)\right]^* = \frac{4}{3}\left[\frac{1}{\omega - (-J-h) + i\delta} - \frac{2}{\omega + h - i\delta}\right], \tag{4.40}$$

with x specifying any of the three existing sites. Only the linear response functions related to spin-flip are non-vanishing. In the RPA case, the non-vanishing non-interacting polarizations are P_{-+}^0 and P_{+-}^0, with the non-vanishing matrix elements:

$$P_{-+}^{0\ xx,xx}(\omega) = -\left[P_{+-}^{0\ xx,xx}(\omega)\right]^* = \frac{4}{3}\left[\frac{1}{\omega - (-\frac{2J}{3} - h) + i\delta} - \frac{2}{\omega + h - i\delta}\right]. \tag{4.41}$$

As $v_{++} = v_{+-} = v_{-+} = v_{--} = 0$, the linear density response function, as computed by the RPA approach, is equal to the non-interacting polarization.

We now consider an Ising model with a triangular lattice of four sites with two sites having two neighbors (site 1,4) and two sites having three neighbors (site 2,3). Choosing $J < 0$ and $-\frac{3J}{16} > h > 0$, the interacting degenerate ground state is two-fold degenerate while the non-interacting degenerate ground state is four-fold degenerate. In the exact

case, the degenerate ground states are the two states where the 1,4 sites have antiparallel spin relative to the 2,3 sites. In the non-interacting case, the degenerate ground states are the four states with zero total spin. The non-vanishing linear density response functions are R_{-+}, R_{+-}, with the non-vanishing matrix elements:

$$R_{-+}^{xx,xx}(\omega) = -\left[R_{+-}^{xx,xx}(\omega)\right]^* = 2\left[\frac{1}{\omega - (-\frac{J}{2} - h) + i\delta} - \frac{1}{\omega + (-\frac{J}{2} + h) - i\delta}\right], \tag{4.42}$$

for sites $x = 2, 3$, and

$$R_{-+}^{xx,xx}(\omega) = -\left[R_{+-}^{xx,xx}(\omega)\right]^* = 2\left[\frac{1}{\omega - (-J - h) + i\delta} - \frac{1}{\omega + (-J + h) - i\delta}\right], \tag{4.43}$$

for sites $x = 1, 4$. In the RPA case, the non-vanishing non-interacting polarizations are P_{-+}^0 and P_{+-}^0, with the non-vanishing matrix elements:

$$\begin{aligned} P_{-+}^{0\ xx,xx}(\omega) = -\left[P_{+-}^{0\ xx,xx}(\omega)\right]^* = &\frac{1}{\omega - (-\frac{7J}{16} - h) + i\delta} + \frac{1}{\omega - (-\frac{3J}{16} - h) + i\delta} \\ &- \frac{1}{\omega - (-\frac{7J}{16} + h) - i\delta} - \frac{1}{\omega - (-\frac{3J}{16} + h) - i\delta}, \end{aligned} \tag{4.44}$$

with x specifying any site of the four sites. As in three-site Ising model, the linear density response function, as computed in the current RPA approach, is equal to the non-interacting polarization.

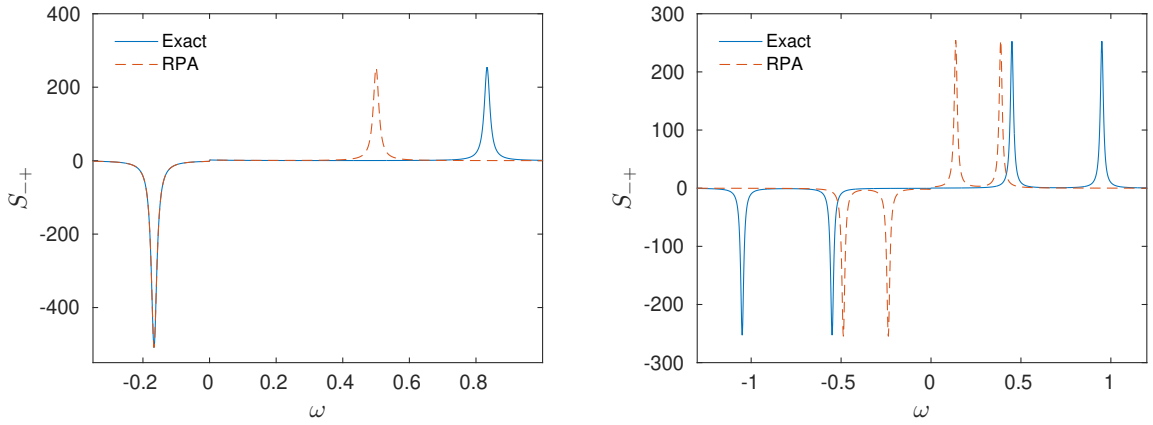

Figure 4.7: The trace $\mathrm{Tr}S_{-+}$ plotted against the energy ω in both the exact case and the ensemble G^0W^0 case for the three-site case with $J = -1$ and $h = 1/6$ (left) and for the four-site case with $J = -1$ and $h = 1/20$ (right), with $\delta = 0.01$. Notice that the spectral response function is not anti-symmetric around $\omega = 0$.

The trace $\mathrm{Tr}S_{-+}$ (identical form for $\mathrm{Tr}S_{+-}$) is plotted as a function of the energy in the three-site case for $J = -1$ and $h = 1/6$ and four-site case for $J = -1$ and $h = 1/20$ in Fig. 4.7. The magnetic field h is thus treated as weak relative the interaction between the spin of neighboring sites. The main peak structure is captured by the RPA approach using MFT for the non-interacting computation, however the peak position is in general predicted to be positioned at too low energies. In the three-site case, the $\omega < 0$ peak is correctly positioned, while the $\omega > 0$ peak is shifted towards $\omega = 0$ with respect to the exact case. In the four-site case, two pairs of peaks are observed, with both pairs being shifted towards $\omega = 0$ with respect to the exact case. MFT is observed to not capture the peak position well for either of the two Ising models with a finite triangular lattice.

4.5 Hydrogen-like atoms

We consider a hydrogen-like atom model occupied by four-electrons. The hydrogen-like atom is composed of a single electron orbiting a nucleus of charge Z. The states are specified by electron configurations given by four quantum numbers: the principle quantum number n, angular momentum quantum number l, magnetic quantum number m_l and spin quantum number m_s. Orbitals of the hydrogen-like atom are known and given by,

$$\phi_{nlm_l}(\mathbf{r}) = R_{nl}(r)Y_{lm_l}(\theta,\varphi), \tag{4.45}$$

where $R_{nl}(r)$ is the radial part and $Y_{lm_l}(\theta,\varphi)$ is the *spherical harmonic*, which gives the angular part. The radial part is of the form:

$$R_{nl}(r) = \sqrt{\left(\frac{2Z}{na_\mu}\right)^3 \frac{(n-l-1)!}{2n\{(n+1)!\}}} e^{-Zr/na_\mu} \left(\frac{2Zr}{na_\mu}\right)^l L^{2l+1}_{n-l-1}\left(\frac{2Zr}{na_\mu}\right), \tag{4.46}$$

with $a_\mu = 4\pi\epsilon_0\hbar^2/\mu e^2$, reduced mass $\mu = m_N m_e/(m_N + m_e)$, nucleus mass m_N and with *generalized Laguerre polynomials* $L^\alpha_n(x)$. The generalized Laguerre polynomials are defined as the solutions of the differential equation:

$$x\frac{d^2L^\alpha_n(x)}{dx^2} + (\alpha+1-x)\frac{dL^\alpha_n(x)}{dx} + nL^\alpha_n(x) = 0. \tag{4.47}$$

As the nucleus mass is much larger than the electron mass ($m_N >> m_e$) the reduced mass is approximately given by $\mu \approx m_e = 1$. We will further work in units such that $4\pi\epsilon_0/e^2 = 1$, and thus a_μ simplifies as $a_\mu \approx 1$.

We consider a four-electron problem, with a restricted space of the hydrogen-like atom system being treated, with only the 1s,2s,2p,3s and 3p orbitals considered. The interaction between the electrons is given by an effective attractive Coulombic interaction of the form $v(\mathbf{r}-\mathbf{r}') = -1/|\mathbf{r}-\mathbf{r}'|$, and thus the considered system is not a model system of an open-shell atom. The interaction elements v_{ijkl} are computed analytically, with the radial and angular part separated by the use of the Laplace expansion:

$$\frac{1}{|\mathbf{r}-\mathbf{r}'|} = \sum_{l=0}^{\infty}\frac{4\pi}{2l+1}\sum_{m=-l}^{l}(-1)^m\frac{r^l_<}{r^{l+1}_>}Y_l^{-m}(\theta,\varphi)Y_l^m(\theta',\varphi'), \tag{4.48}$$

with $r_< = \min(r,r')$ and $r_> = \max(r,r')$. The angular integration can be solved by the use of the orthogonality of the spherical harmonics. The radial integration corresponds to two integrations over a polynomial multiplied by an exponential, and can thus be solved analytically by known formulae. An alternative approach, which is not used in the current thesis, is to treat the v_{ijkl} elements as parameters instead.

In the considered four-electron problem, the interacting ground state is non-degenerate. The non-interacting ground state is nine-fold degenerate, as computed with the self-consistent ensemble Hartree potential, with the states corresponding to all states with configuration $1s^22p^2$. A non-ensemble G^0W^0 computation, of the non-ensemble B approach form introduced in section 4.3, will be considered in addition to the ensemble G^0W^0 and the exact computations.

The TrS and TrA are computed and plotted as functions of the energy for $Z = 1$ and $Z = 4$, both shown in Fig. 4.8, in the ensemble and non-ensemble G^0W^0 approaches as well as the exact approach. The observations are however quite similar for both values of

Z. The peak structure of TrS in the ensemble G^0W^0 approach is, with exception of the neglected low ω peaks, in better agreement with the exact result. For $Z = 1$ and $Z = 4$ the exact peaks above $\omega = 0.3$ and $\omega = 1$, respectively, are shifted towards higher energies in the approximate approaches, however the main structures are in good agreement. The one exception is the peak a bit below $\omega = 6$ in the case of $Z = 4$, where the peak position is in better agreement. The trace TrA is well in agreement in both approximate approaches with the exact one, capturing the five and six major peak structures and their positions for $Z = 1$ and $Z = 4$, respectively. However, the finer detail of each peak structure varies relative the exact case for certain peak structures. In Fig. 4.8, the single peak at the electron affinity in the exact case is in reality two peaks very close to each other. Thus the approximate approaches significantly overestimate the splitting of the peaks at the electron affinity.

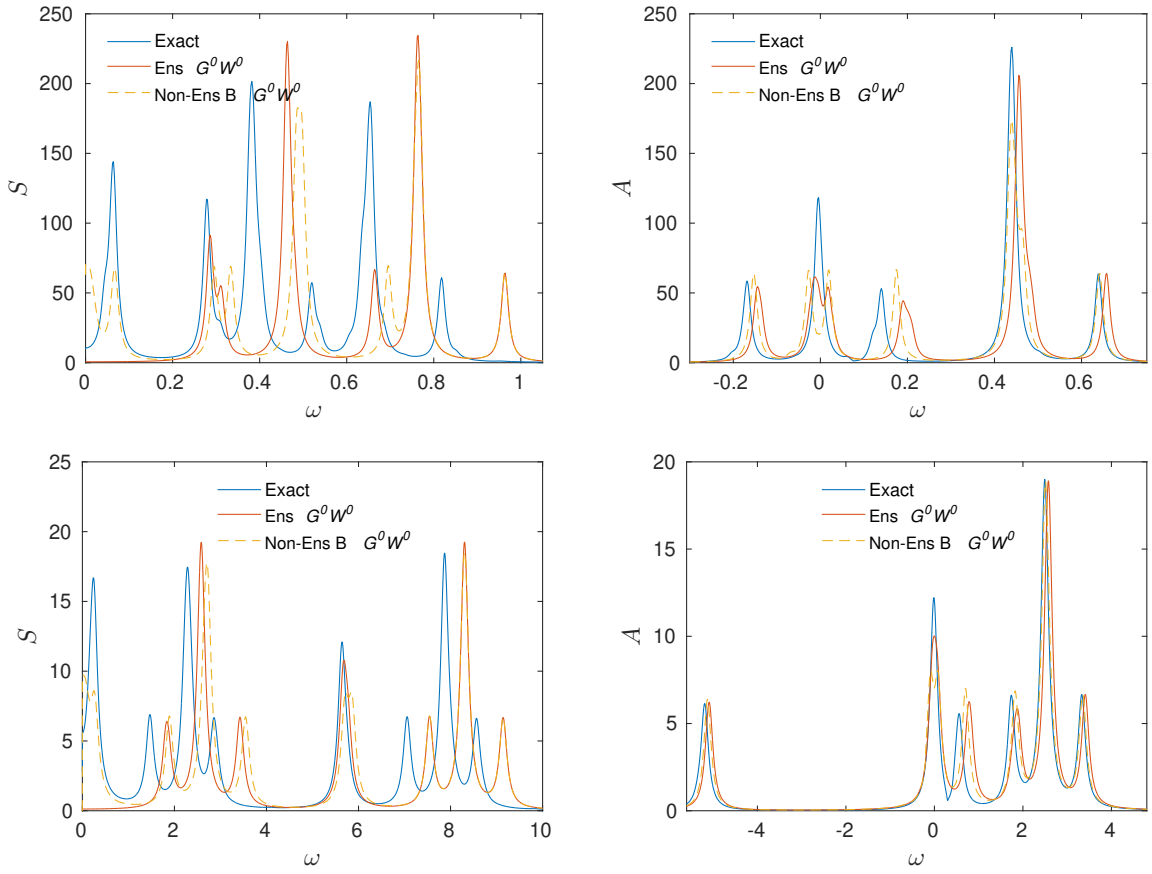

Figure 4.8: The TrS (left row) and TrA (right row) plotted against the energy ω in the exact approach, and the ensemble and non-ensemble G^0W^0 approaches, with $Z = 1$ and $\delta = 0.01$ (upper row) and $Z = 4$ and $\delta = 0.1$ (lower row). The spectral response function is anti-symmetric around $\omega = 0$.

The application of the ensemble formalism shows encouraging results for more complex system, with the main structures of both the response and spectral function being captured, with also the peak positions being well in agreement with exact results in the latter. As observed in the Hubbard model, peaks originating from the breaking of the degeneracy are observed to not be captured in the ensemble approach as expected from earlier discussions. As the form of the Green's function is captured well, however, we expect a self-consistent computation to capture the response function well.

Chapter 5

Conclusion

We have proposed and developed an ensemble Green's function theory for systems of interacting electrons with degenerate ground states based on the density matrix formalism. The theory is built upon an ensemble Green's function G, containing the ensemble analogues information found in the usual zero-temperature Green's function for electronic systems with non-degenerate ground states, and auxiliary Green's functions G_n. An exact set of self-consistent equations for the G_n Green's functions, corresponding to the ensemble analogue of the Hedin equations, were derived. By employing a diagonalization procedure, we then showed that the relations between the time-ordered and retarded linear response function are satisfied by an introduced ensemble response function. An ensemble analogue of the GWA was proposed, and within the approximation a one-shot ensemble G^0W^0 approach and self-consistent ensemble GW approach were constructed.

A comparison between the ensemble and temperature formalisms were made in the limit of $T \to 0^+$. In this limit, the real-time Green's function acquires the form of the ensemble Green's function. An extension of the temperature formalism to electronic systems with degenerate states was further proposed. A form of the time-ordered real-time response function allowing for the diagonalization procedure and with a natural connection to the retarded real-time response function was developed. A modification of the Matsubara Green's function $\mathcal{G}$ was proposed, allowing for the computation of this time-ordered response function by the use of auxiliary Matsubara Green's functions $\mathcal{G}_n$. In the limit of $T \to 0^+$, the real-time linear density response function was found to acquire the form of the zero-temperature analogue in the proposed ensemble formalism. This relation validates the extension, diplaying that it contains the proposed ensemble Green's function theory.

The ensemble formalism was applied to four model systems: a Hubbard model, a two-dimensional harmonic oscillator, an Ising model and a hydrogen-like system. A problem which arises in the ensemble G^0W^0 approach, is that the peaks in the response function originating from the transitions between states in the degenerate subspace in the mean-field ensemble Hamiltonian are absent with the employment of the diagonalization scheme. This aspect was, for example, observed in the analytically solvable three-orbital Hubbard model. The diagonalization procedure cannot account for the problem, as it simply corresponds to rotating the degenerate ground states in the degenerate subspace. We argue instead that the problem originates from the mean-field approach not capturing the mechanics of the system, for example the repulsive/attractive nature of the interaction in the Hubbard model. The removal of peaks originating from the breaking of degeneracy going from the non-interacting to interacting states. The possibility of degeneracy break-

ing is only first incorporated in the computation of the self-energies Σ_n, and we therefore expect this issue to be solved in a self-consistent computational scheme.

Treatment of the Ising model with a triangular lattice gave an example of the application of the formalism to simple frustrated systems. It further illustrated the ensemble form of the linear charge and magnetic response function and polarization. It was observed that the MFT did not capture the peak position well in the ensemble G^0W^0 approach for either of the considered Ising models with a finite triangular lattice.

The remaining two model systems illustrated the application of the proposed formalism to more complex systems. Both systems gave examples of a complete breaking of the groundstate degeneracy in the transition from a non-interacting to interacting system. In both systems the ensemble case was compared to the exact case and non-ensemble case. In the two-dimensional harmonic oscillator, the exact structure was observed to be captured in the ensemble case as well as in the non-ensemble case. In contrast to the well-defined ensemble approach, the non-ensemble approaches are ill-defined, as ignoring the degeneracy is ill-defined. The hydrogen-like system was treated, with the ensemble and non-ensemble G^0W^0 approaches in reasonable agreement with the peak structure of the exact approach in both the spectral form of the linear response function and the spectral function, with the ensemble G^0W^0 approach being in better agreement.

All four models motivate the ensemble formalism as a well-defined and reasonable approach for many-electron systems with degenerate ground states, capturing to a large extent the exact results in our current considerations. Our considerations have been mainly for an ensemble one-shot G^0W^0 computational scheme. As in the standard G^0W^0 approach, the agreement is perceived to be better for initial non-interacting energies and states close to the interacting ones, leading to worse results in the Ising model relative the other three models as well as worse result for the Hubbard model with $U = 0.3$ then $U = 0.1$. A general problem in the one-shot approach, is the problem of the removal of peaks arising from the breaking of the degeneracy going from the non-interacting to interacting states. Beyond a better choice of mean-field approach, capturing the energy structure of a system, a self-consistent approach is expected to solve this issue. Our proposed ensemble Green's function formalism for general treatment of electron system with degenerate ground states allows for simulation of a large class of systems and materials, giving a well-defined and unique solution.

Chapter 6

Outlook

The proposed ensemble Green's function theory allows for treatment of realistic electronic systems with degenerate ground states using a well-defined Green's function method. We plan to publish a paper based on the work done in this Master thesis. In the current thesis, only model systems were considered, and thus realistic systems such as open-shell atoms are planned to be studied in the future. Further plans exists for developing an ensemble analogue of the self-consistent QSGW scheme and to apply it to model systems to, for example, study if the peaks removed by the diagonalization procedure appears naturally and in agreement with exact results. A general benchmarking of the ensemble one-shot G^0W^0 and self-consistent GW for a range of different systems would be of general interest to study the limitations and strengths of the ensemble formalism.

A finite-temperature Green's function theory was proposed, however no explicit computations using the formalism has been considered. For future developments, employing the proposed finite-temperature formalism to model and realistic systems with degenerate states would enlighten the range of predictivity of the formalism. An apparent computational problem with the proposed finite-temperature formalism is the drastically increased computational cost of computing the separate self-energies for each states. It would thus be of interest to pursue a finite-temperature Green's function formalism which separates the treatment of the degenerate and non-degenerate subspaces.

Small finite systems with smaller degeneracy were considered, however in macroscopic systems with potentially larger degeneracy, computational cost associated with the approach would increase. An important type of system which display large degeneracy is frustrated systems. The macroscopic degeneracy in spin ice, related to the disorder of the system, would lead, with naive application of the ensemble G^0W^0 approach, to unfeasible computational cost. The symmetry of the system is expected to lead to multiple G_n computations of identical structure. It would therefore be of interest to pursue development of a method which exploits the symmetry of a system, allowing for only a subsection of the degenerate ground states to be considered. By computing the appropriate weights for each Green's function G_n, the ensemble Green's function could thus be possible to be computed with a decreased computational cost.

Appendices

Appendix A

Spectral representation of the Green's function

The spectral representation of the Green's function (Eq.(2.36)) will be derived here. Working in the Heisenberg picture, the Green's function, defined in Eq. (2.32), can be rewritten as:

$$\begin{aligned} G(1,2) =& -i\theta(t_1-t_2)\langle\Psi_0|\hat{\psi}(1)\hat{\psi}^\dagger(2)|\Psi_0\rangle + i\theta(t_2-t_1)\langle\Psi_0|\hat{\psi}(1)\hat{\psi}^\dagger(2)|\Psi_0\rangle \\ =& -i\theta(t_1-t_2)\sum_m \langle\Psi_0|\hat{\psi}(r_1)|\Psi_m\rangle\langle\Psi_m|\hat{\psi}^\dagger(r_2)|\Psi_0\rangle e^{-i(t_1-t_2)(E_m-E_0)} \\ &+ i\theta(t_2-t_1)\sum_m \langle\Psi_0|\hat{\psi}^\dagger(r_2)|\Psi_m\rangle\langle\Psi_m|\hat{\psi}(r_1)|\Psi_0\rangle e^{i(t_1-t_2)(E_m-E_0)}, \end{aligned} \tag{A.1}$$

where $\theta(t_1-t_2)$ is the Heaviside function and the sum m is over all states spanning the Hamiltonian. Here we have used the time-independence of the Hamiltonian, observing that it leads to the Green's function only depending on the time-difference t_1-t_2, as mentioned in section 2.5. One can represent the Heaviside function as a contour integral of the form:

$$\theta(t_1-t_2) = -\int_{-\infty}^{\infty}\frac{d\omega}{2\pi i}\frac{e^{-i\omega(t_1-t_2)}}{\omega+i\delta}, \tag{A.2}$$

with δ being an infinitesimal positive constant. The frequency space Green's function can now be constructed, by using Eq. (2.26) and the residue theorem for simple poles, as:

$$\begin{aligned} G(1,2;\omega) =& \, i\int_0^\infty d\tau\left[\sum_m \langle\Psi_0|\hat{\psi}(r_1)|\Psi_m\rangle\langle\Psi_m|\hat{\psi}^\dagger(r_2)|\Psi_0\rangle e^{i(\omega-(E_m-E_0)+i\delta)\tau}\right] \\ &- i\int_{-\infty}^0 d\tau\left[\sum_m \langle\Psi_0|\hat{\psi}^\dagger(r_2)|\Psi_m\rangle\langle\Psi_m|\hat{\psi}(r_1)|\Psi_0\rangle e^{i(\omega+(E_m-E_0)-i\delta)\tau}\right] \\ =& \sum_m \frac{\langle\Psi_0^N|\hat{\psi}^\dagger(2)|\Psi_m^{N-1}\rangle\langle\Psi_m^{N-1}|\hat{\psi}(1)|\Psi_0^N\rangle}{\omega+E_m^{N-1}-E_0^N-i\delta} \\ &+ \sum_m \frac{\langle\Psi_0^N|\hat{\psi}(1)|\Psi_m^{N+1}\rangle\langle\Psi_m^{N+1}|\hat{\psi}^\dagger(2)|\Psi_0^N\rangle}{\omega-E_m^{N+1}+E_0^N+i\delta}, \end{aligned} \tag{A.3}$$

where in the last step, one has used that the number of electrons in the ground state is N and thus the connected excited states needs to have $N-1$ and $N+1$ number of electrons respectively. The sought Eq. (2.36) has thus been derived.

Appendix B

Functionals

The *functional* concept is of general importance in physics, and is used in the Schwinger functional derivative technique in the development of the Green's function formalism. The class of functionals considered in this thesis can be considered as functions of functions. Onwards our use of functional will only specify this class of functionals.

A functional is similar to a function. A many-variable function $f(r_1, r_2, ..., r_n)$ gives a number for a set of numbers $\{r_i, i = 1, ..., n\}$. Similarly, a functional $F[\phi_1(r), ..., \phi_n(r)]$ gives a number for a set of functions $\{\phi_i(r), i = 1, ..., n\}$. By the introduction of the functional derivative $\delta F[\phi(r)]/\delta\phi(r')$, the functional can be written as,

$$F[\phi(r)] \equiv \int dr' \frac{\delta F[\phi(r)]}{\delta\phi(r')}\phi(r'). \tag{B.1}$$

The mathematical rigourus definition of the functional derivative is

$$\frac{\delta F[\phi(r)]}{\delta\phi(r')} \equiv \lim_{\epsilon\to 0} \frac{F[\phi(r') + \epsilon\delta(r - r')] - F[\phi(r')]}{\epsilon}. \tag{B.2}$$

As an example, consider the function, which itself is a functional satisfying the relation

$$\phi(r) = \int dr' \delta(r - r')\phi(r'). \tag{B.3}$$

The functional derivative of the function is thus:

$$\frac{\delta\phi(r)}{\delta\phi(r')} = \delta(r - r'). \tag{B.4}$$

In pratice the functional derivative is analogous to the partial derivative. An analogus chain-rule for functional derivatives, as for multi-variable functions, exists and is of the form:

$$\frac{\delta F[\rho[\phi(r)]]}{\delta\phi(r')} = \int dr'' \frac{\delta F[\rho(r)]}{\delta\rho(r'')} \frac{\delta\rho[\phi(r'')]}{\delta\phi(r')}, \tag{B.5}$$

where ρ is a functional of the function ϕ.

Appendix C

Linear response theory derivations

The current appendix collects derivations related to the linear response theory used in the thesis.

C.1 Zero-temperature: Linear density response function

A derivation of Eq. (2.65) in section 2.5 will now be given. An external perturbative potential is assumed to be of the form (2.20). Employing a Schwinger functional derivative technique approach, the linear density response function can be derived. For more information regarding the response function at zero temperature see for example [28].

Using Eqs. (2.34), (2.50) and (2.63) the linear density response function can be written in the form:

$$\begin{aligned} R(1,2) &= -i\frac{\delta G(1,1^+)}{\delta\varphi(2)}\bigg|_{\varphi=0} \\ &= -i\left(-\langle\Psi_0|\hat{\rho}_H(1)|\Psi_0\rangle\langle\Psi_0|\hat{\rho}_H(2)|\Psi_0\rangle + \langle\Psi_0|T[\hat{\rho}_H(1)\hat{\rho}_H(2)]|\Psi_0\rangle\right) \\ &= -i\langle\Psi_0|T[\Delta\hat{\rho}_H(1)\Delta\hat{\rho}_H(2)]|\Psi_0\rangle, \end{aligned} \tag{C.1}$$

where $\Delta\hat{\rho}$ is defined in Eq. (2.25). The spectral representation of Eq. (C.1) can be obtained in a scheme similar to the ones used to derive the form of the frequency space Green's function in Appendix A. Assuming the Hamiltonian is time-independent, Eq. (C.1) can be rewritten as:

$$\begin{aligned} R(1,2) =& -i\theta(t_1-t_2)\langle\Psi_0|\Delta\hat{\rho}_H(1)\Delta\hat{\rho}_H(2)|\Psi_0\rangle - i\theta(t_2-t_1)\langle\Psi_0|\Delta\hat{\rho}_H(2)\Delta\hat{\rho}_H(1)|\Psi_0\rangle \\ =& -i\theta(t_1-t_2)\sum_m\langle\Psi_0|\Delta\hat{\rho}_H(1)|\Psi_m\rangle\langle\Psi_m|\Delta\hat{\rho}_H(2)|\Psi_0\rangle e^{-i(t_1-t_2)(E_m-E_0)} \\ & -i\theta(t_2-t_1)\sum_m\langle\Psi_0|\Delta\hat{\rho}_H(2)|\Psi_m\rangle\langle\Psi_m|\Delta\hat{\rho}_H(1)|\Psi_0\rangle e^{i(t_1-t_2)(E_m-E_0)}, \end{aligned} \tag{C.2}$$

where $\theta(t_1-t_2)$ is the Heaviside function and the sum m is over all states spanning the Hamiltonian. The time-independence of the Hamitonian leads to time-dependence of the linear density response function entering as t_1-t_2. Representing the Heaviside function as a contour integral of the form:

$$\theta(t_1-t_2) = -\int_{-\infty}^{\infty}\frac{d\omega}{2\pi i}\frac{e^{-i\omega(t_1-t_2)}}{\omega+i\delta}, \tag{C.3}$$

with δ being an infinitesimal positive constant, the spectral representation of the linear density response function can be written as:

$$\begin{aligned} R(1,2;\omega) &= i\int_0^\infty d\tau \left[\sum_m \langle\Psi_0|\Delta\hat{\rho}(1)|\Psi_m\rangle\langle\Psi_m|\Delta\hat{\rho}(2)|\Psi_0\rangle e^{i(\omega-(E_m-E_0)+i\delta)\tau}\right] \\ &+ i\int_{-\infty}^0 d\tau \left[\sum_m \langle\Psi_0|\Delta\hat{\rho}(2)|\Psi_m\rangle\langle\Psi_m|\Delta\hat{\rho}(1)|\Psi_0\rangle e^{i(\omega+(E_m-E_0)-i\delta)\tau}\right] \\ &= \sum_{m\neq 0}\left[\frac{\langle\Psi_0|\hat{\rho}(1)|\Psi_m\rangle\langle\Psi_m|\hat{\rho}(2)|\Psi_0\rangle}{\omega-E_m+E_0+i\delta} - \frac{\langle\Psi_0|\hat{\rho}(2)|\Psi_m\rangle\langle\Psi_m|\hat{\rho}(1)|\Psi_0\rangle}{\omega+E_m-E_0-i\delta}\right]. \end{aligned} \tag{C.4}$$

The sought Eq. (2.65) has thus been derived.

C.2 Finite-temperature: Linear density response function

The Eqs. (2.93) and (2.95) in section 2.6 will be derived in the current section. As in the previous section, the external perturbative potential is assumed to be of the form (2.20). In the current section, instead of the Schwinger functional derivative approach, the Kubo approach of deriving the linear response function will be used. For more information regarding the response function finite temperature see for example [28].

The first-order change in the ensemble average of the density is given by:

$$\delta\langle\hat{\rho}(r,t)\rangle = i\int_{t_0}^t dt' \mathrm{Tr}\left\{\hat{\rho}_G[\hat{\phi}_K(t'),\hat{\rho}_K(r,t)]\right\}. \tag{C.5}$$

Using the structure of the perturbative potential, assumed to be of the form (2.20), one obtaines the change in the ensemble average of the density as:

$$\delta\rho(r,t) = i\int d^3r'\int_{t_0}^t dt'\varphi(r't')\mathrm{Tr}\left\{\hat{\rho}_G[\hat{\rho}_K(r',t'),\hat{\rho}_K(r,t)]\right\}. \tag{C.6}$$

The retarded linear density response function R^R is defined by

$$\delta\langle\hat{\rho}(r,t)\rangle = \int_{t_0}^t dt'\int d^3r' R^R(rt,r't')\varphi(r't'), \tag{C.7}$$

with the special case of the change of the ground state expectation value at zero-temperature previously treated in Eq. (2.22). The form of R^R can thus be identified, by a comparison between (C.6) and (C.7), as:

$$iR^R(rt,r't') \equiv \mathrm{Tr}\left\{\hat{\rho}_G[\hat{\rho}(r,t),\hat{\rho}(r',t')]\right\}\theta(t-t'). \tag{C.8}$$

The standard rewritten form of the retarded linear response function is the following one:

$$iR^R(rt,r't') \equiv \mathrm{Tr}\left\{\hat{\rho}_G[\Delta\hat{\rho}(r,t),\Delta\hat{\rho}(r',t')]\right\}\theta(t-t'), \tag{C.9}$$

with $\Delta\hat{\rho}$ defined by Eq. (2.94), which is the sought Eq. (2.93).

As in section 2.4, the time-ordered linear density response function is required to satisfy the relations (2.28) and (2.29). The time-ordered linear density response function satisfying these relations can be constructed as:

$$iR(1,2) \equiv \mathrm{Tr}\left\{\hat{\rho}_G T\left[\hat{\rho}(1)\hat{\rho}(2)\right]\right\}, \tag{C.10}$$

with non-degenerate states assumed. The spectral representation of Eq. (C.10) can be derived similar to the zero-temperature one, derived in the previous section. Assuming the Hamiltonian is time-independent, Eq. (C.10) can be rewritten as:

$$\begin{aligned} iR(1,2) &= {Z_G}^{-1}\sum_n \left[e^{-\beta K_n}\langle\Psi_n|\hat{\rho}(1)\hat{\rho}(2)|\Psi_n\rangle\theta(t_1-t_2) + e^{-\beta K_n}\langle\Psi_n|\hat{\rho}(2)\hat{\rho}(1)|\Psi_n\rangle\theta(t_2-t_1)\right] \\ &= {Z_G}^{-1}\sum_{n,m}\left[e^{-\beta K_n}\theta(t_1-t_2) + e^{-\beta K_m}\theta(t_2-t_1)\right] \\ &\times \langle\Psi_n|\hat{\rho}(r_1)|\Psi_m\rangle\langle\Psi_m|\hat{\rho}(r_2)|\Psi_n\rangle e^{-i(t_1-t_2)(K_m-K_n)}, \end{aligned} \tag{C.11}$$

where the sum over n, m is over all states. Notice the time-dependence enters as $t_1 - t_2$, as stated in section 2.6. Representing the Heaviside function as a contour integral of the form (C.3), the spectral representation of the linear density response function can be written as:

$$\begin{aligned} R(1,2;\omega) &= {Z_G}^{-1}\sum_{n,m}\langle\Psi_n|\Delta\hat{\rho}(1)|\Psi_m\rangle\langle\Psi_m|\Delta\hat{\rho}(2)|\Psi_n\rangle \\ &\times\left[\frac{e^{-\beta K_n}}{\omega - K_m + K_n + i\delta} - \frac{e^{-\beta K_m}}{\omega - K_m + K_n - i\delta}\right]. \end{aligned} \tag{C.12}$$

This is of an identical form as the sought Eq. (2.95), and thus Eqs. (2.93) and (2.95) have been derived.

C.3 Ising model: Linear charge and magnetic response function

A derivation of Eq. (4.37) in section 4.4 will now be given. An external perturbative potential is assumed to be of the form (4.31). The following derivation will be similar to the one given for the linear ensemble density response function.

Using Eqs. (4.32) and (4.35), and the Schwinger functional derivative approach, the linear charge and magnetic response function can be written in the form:

$$\begin{aligned} R_{ij}(1,2) &= \left.\frac{\delta\langle\hat{\sigma}^i(1)\rangle}{\delta\varphi_j(2)}\right|_{\varphi_j=0} \\ &= -i\frac{1}{M}\sum_{n=1}^{M}\langle\Psi_n|T[\Delta\hat{\sigma}^i_{nH}(1)\Delta\hat{\sigma}^j_{nH}(2)]|\Psi_n\rangle \end{aligned} \tag{C.13}$$

with $\Delta\hat{\sigma}^i_n$ defined by:

$$\Delta\hat{\sigma}^i_n(1) = \hat{\sigma}^i - \langle\Psi_n|\hat{\sigma}^i|\Psi_n\rangle. \tag{C.14}$$

Assuming the Hamiltonian is time-independent and using the representation of the Heaviside function as a contour integral of the form (C.3), the linear charge and magnetic

response function can be written in the ensemble form as:

$$R_{ij}(1,2;\omega) = \frac{1}{M}\sum_{n=1}^{M}\sum_{m\neq n}^{\text{exci}}\left[\frac{\langle\Psi_n|\hat{\sigma}^i(1)|\Psi_m\rangle\langle\Psi_m|\hat{\sigma}^j(2)|\Psi_n\rangle}{\omega - E_m + E_0 + i\delta} - \frac{\langle\Psi_n|\hat{\sigma}^j(2)|\Psi_m\rangle\langle\Psi_m|\hat{\sigma}^i(1)|\Psi_n\rangle}{\omega + E_m - E_0 - i\delta}\right]. \tag{C.15}$$

Employing the diagonalization procedure proposed in section 3.1, the linear charge and magnetic response function can be rewritten as:

$$R_{ij}(1,2;\omega) = \frac{1}{M}\sum_{n=1}^{M}\sum_{m}^{\text{exci}}\left[\frac{\langle\Psi_n|\hat{\sigma}^i(1)|\Psi_m\rangle\langle\Psi_m|\hat{\sigma}^j(2)|\Psi_n\rangle}{\omega - E_m + E_0 + i\delta} - \frac{\langle\Psi_n|\hat{\sigma}^j(2)|\Psi_m\rangle\langle\Psi_m|\hat{\sigma}^i(1)|\Psi_n\rangle}{\omega + E_m - E_0 - i\delta}\right], \tag{C.16}$$

which is the sought Eq. (4.37).

Bibliography

[1] H. L. Störmer, "Nobel Lecture: The fractional quantum Hall effect", Rev. Mod. Phys. **71**, 875 (1999).

[2] L. Balents, Nature **464**, 199 (2010).

[3] S. T. Bramwell and M. J. P. Gingras, Science **294**, 1495–1501 (2001).

[4] P. Hohenberg and W. Kohn, Phys. Rev. **136**, B864 (1964).

[5] W. Kohn and L. J. Sham, Phys. Rev. **140**, A1133 (1965).

[6] V. I. Anisimov, J. Zaanen, and O. K. Andersen, Phys. Rev. B **44**, 943 (1991).

[7] V. I. Anisimov, I. V. Solovyev, M. A. Korotin, M. T. Czyżyk, and G. A. Sawatzky, Phys. Rev. B **48**, 16929 (1993).

[8] A. I. Lichtenstein, V. I. Anisimov, and J. Zaanen, Phys. Rev. B **52**, R5467(R) (1995).

[9] A. Svane and O. Gunnarsson, Phys. Rev. Lett. **65**, 1148 (1990).

[10] V.I. Anisimov, A. Poteryaev, M. Korotin, A. Anokhin and G. Kotliar, J. Phys.: Condens. Matter **9**, 7359 (1997).

[11] A. I. Liechtenstein, and M. I. Katsnelson, Phys. Rev. B **57**, 6884 (1998).

[12] A. Georges, and G. Kotliar, Phys. Rev. B **45**, 6479 (1992).

[13] A. Georges, G. Kotliar, W. Krauth, and M. J. Rozenberg, Rev. Mod. Phys. **68**, 13 (1996).

[14] L. Hedin, 1965a Phys. Rev. **139**, A796 (1965).

[15] U. von Barth, and B. Holm, Phys. Rev. B **54**, 8411 (1996); Erratum Phys. Rev. B **55**, 10120 (1997).

[16] T. Kotani, M. van Schilfgaarde, and S. V. Faleev, Phys. Rev. B **76**, 165106 (2007).

[17] S. Biermann, F. Aryasetiawan, and A. Georges, Phys. Rev. Lett. **90**, 086402 (2003).

[18] Y. Ma, M. Rohlfing, and A. Gali, Phys. Rev. B **81**, 041204 (R) (2010).

[19] C. Attaccalite, M. Bockstedte, A. Marini, A. Rubio, and L. Wirtz, Phys. Rev. B **83**, 144115 (2011).

[20] E. L. Shirley and R. M. Martin, Phys. Rev. B **47**, 15 404 (1993).

[21] J. Lischner, J. Deslippe, M. Jain, S. G. and Louie, Phys. Rev. Lett. **109**, 036406 (2012).

[22] A. J. Layzer, Phys. Rev. **129**, 897 (1962).

[23] L. S. Cederbaum and J. Schirmer, Z. Physik **271**, 221 (1974).

[24] C. Boulder, G. Panati, and G. Stoltz, Phys. Rev. Lett. **103**, 230401 (2009).

[25] J. J. Sakurai, J. Napolitano, *Modern Quantum Mechanics*, Second edition (Pearson, 2011).

[26] G. Mahan, *Many-Particle Physics*, Second edition (Plenum Press, 1990).

[27] M. Gell-Mann and F. Low, Phys. Rev. **84**, 350 (1951).

[28] A. L. Fetter and J. D. Walecka, *Quantum Theory of Many-Particle Systems*, (McGraw-Hill, 1971).

[29] F. Aryasetiawan and O. Gunnarson, Rep. Prog. Phys. **61**, 237 (1998).

[30] ARPESgeneral (https://commons.wikimedia.org/wiki/File:ARPESgeneral.png), public domain

[31] E. K. U. Gross, E. Runge and O. Heinonen, *Many-Particle Theory*, (IOP Publishing, 1991).

[32] V.I. Anisimov *et al*, *Strong Coulomb Correlations in Electronic Structure Calculations*, (Gordon and Breach Science Publishers, 2000).

[33] F. Aryasetiawan, and S. Biermann, Phys. Rev. Lett. **100**, 116402 (2008).

[34] J. Hubbard, Proceedings of the Royal Society of London. Series A. Mathematical and Physical Sciences **276**, 1365 (1963).

[35] G.H. Wannier, Phys. Rev. **79**, 357 (1950).